TATION PAGE

Form Approved
OMB No. 0704-0188

1. AGENCY USE ONLY (Leave blank)	2. REPORT DATE	3. REPORT TYPE AND DATES COVERED
	1/31/92	Final 12/1/89 to 1/30/91

4. TITLE AND SUBTITLE
Steady and Transient Analysis of Flows Exhibiting Strong Viscous/Inviscid Interaction (Composite RNS Procedures)

5. FUNDING NUMBERS
G:AFOSR-90-0096

6. AUTHOR(S)
Stanley G. Rubin
Prem K. Khosla

7. PERFORMING ORGANIZATION NAME(S) AND ADDRESS(ES)
Dept. of Aerospace Engineering and Engineering Mechanics
Mail Location 343
University of Cincinnati
Cincinnati, Ohio 45221-0343

8. PERFORMING ORGANIZATION REPORT NUMBER
AFOSR-TR- 92 0164
N/A

9. SPONSORING/MONITORING AGENCY NAME(S) AND ADDRESS(ES)
Air Force Office of Scientific Research
Building 410
Bolling AFB, DC 20332
NA

10. SPONSORING/MONITORING AGENCY REPORT NUMBER
AFOSR-90-0096
2307/A5

11. SUPPLEMENTARY NOTES

12a. DISTRIBUTION/AVAILABILITY STATEMENT
"Original contains color plates: All DTIC reproductions will be in black and white"
Approved for public release; distribution unlimited

12b. DISTRIBUTION CODE

13. ABSTRACT (Maximum 200 words)

The Reduced Navier-Stokes (RNS) formulation for viscous-inviscid interacting flows with significant upstream or 'elliptic' effects has been applied for transient flows in inlets and steady two and three dimensional flows over cone-cylinder flare, afterbody and channel configurations. The solution technique allows for shock-boundary layer interaction and for regions of axial and secondary flow recirculation. It has been demonstrated that for laminar flows there exists a critical Reynolds number above which the solution exhibits a breakdown. This behavior, which occurs in the region of recirculation and can be correlated with the transition location, is grid dependent and can be missed with insufficiently refined grids or when artificial viscosity is introduced. The pressure-split RNS procedure is a special form of flux-vector splitting that has very favorable properties for sharp shock-shock and shock-boundary layer interaction. A sparse matrix direct solver procedure has been applied for both two dimensional transient flows, and for three dimensional steady flows. A domain decomposition multigrid procedure has further developed for viscous interacting flows, where significant grid stretching is required in discrete flow regions.

14. SUBJECT TERMS	15. NUMBER OF PAGES
Reduced Navier Stokes, Three-Dimensional Separation, Multigrid, Transient, Viscous Interaction, Shock Interaction, Domain Decomposition	51
	16. PRICE CODE

17. SECURITY CLASSIFICATION OF REPORT	18. SECURITY CLASSIFICATION OF THIS PAGE	19. SECURITY CLASSIFICATION OF ABSTRACT	20. LIMITATION OF ABSTRACT
Unclassified	Unclassified	Unclassified	UL

FINAL REPORT

COMPOSITE REDUCED NAVIER-STOKES PROCEDURES FOR FLOW PROBLEMS WITH STRONG PRESSURE INTERACTIONS

December 1, 1989 through November 30, 1991

AFOSR Grant No. 90-0096

Principal Investigators:

S.G. Rubin

P.K. Khosla

Department of Aerospace Engineering and Engineering Mechanics

University of Cincinnati

Cincinnati, Ohio 45221-0343

1. Introduction

The purpose of this AFOSR research program was the development and application of primitive variable composite velocity and pressure flux-vector splitting formulations that allow for efficient numerical evaluation and prediction of viscous interacting flows. Three-dimensional separated flows over cone-cylinder-flare and afterbody configurations, shock-shear/boundary layer interaction, high frequency laminar flow breakdown and transitional behavior, and unsteady viscous/inviscid interactions associated with regions of flow reversal and shock boundary layer coupling, as occur in supersonic inlets and in corner regions, are the primary topic areas.

A reduced form of the Navier Stokes equations, termed here RNS, is the foundation for all formulations. The RNS system is a composite of the full Euler and boundary layer/triple deck models. The flux-splitting or composite velocity procedures are designed to optimize the numerical representations of viscous and inviscid regions, respectively. These techniques can be viewed as a composite or single system 'matched interacting boundary layer-inviscid flow' solver or as a full elliptic version of parabolized Navier Stokes or PNS methodology. Both methods are applicable across the entire mach number range, i.e. from incompressible to hypersonic, and the same code has been applied at both ends of the spectrum.

These formulations have been shown to be applicable to a high degree of accuracy for (a) flows with moderate to large regions of axial and secondary flow reversal, for (b) capturing sharp shock wave interactions and contact discontinuities, and (c) for steady and transient behavior associated with shock-boundary layer interaction. The RNS system has also been shown to accurately represent the full NS system for this class of flow problems, and, with a deferred corrector procedure, full NS solutions can be recovered. The RNS procedure allows for simplification of numerical boundary conditions and does not require the introduction of added artificial viscosity in shock and strong pressure interaction regions. This

allows for fine mesh calculations that minimize numerical viscous effects, which can overwhelm the influence of physical viscosity with large transient effects, in reverse flow regions, and with shock-boundary layer interaction.

Several solution procedures for the discrete system of quasilinearized equations have been applied. For steady flow, space marching global relaxation techniques have been demonstrated successfully for both the pressure variable flux-split and composite velocity formulations. For fully supersonic conditions or for very large free stream mach numbers, where subsonic viscous layers are very thin and where the effects of geometry do not have a significant influence on the axial flow behavior, a single pass will suffice to obtain the exact or a very good approximate solution. For subsonic or transonic flows, a multiple pass or full relaxation strategy is required.

For fine meshes, a unidirectional or semi-coarsening multigrid strategy, that is particularly effective when full multigrid methods fail, as with significant grid stretching, and a sparse matrix direct solver strategy, that is particularly effective for very strong interactions occuring in very local domains, where relaxation methods fail or stall, have been representd. These are currently being applied for two-dimensional transient and three dimensional steady computations with reverse flow and shock-boundary-layer interactions.

Specific problem areas under investigation include (a) three-dimensional separated flows on afterbody or boattail geometries, (b) transient viscous flows in supersonic inlets, (c) shock-boundary-layer interaction in supersonic flows along compression ramps and over cone-cylinder-flare configurations; high temperature wall and real gas effects are under consideration. These flows involve shock-boundary-layer, shock-shock and transient shock boundary-layer interactions and exhibit large regions of confined flow reversal and in some cases vortex breakup.

The following topic areas have been presented during the period of the grant. The references in brackets are given in section 5

Pressure Relaxation and Flux Vector Splitting [1,13,16,17,20,23-25]

Semi-coarsening Multigrid/Laminar Flow Breakdown [9,13,23-25]

Multigrid Domain Decomposition [23-25]

Transient (RNS) Supersonic Inlet Unstart/Restart and Diffuser Flow [1-5,8-11,14,17,26]

Sparse Matrix Solvers for Complex Viscous Interactions [8-11,14,15]

Blunt Body Considerations [16,18]

Supersonic Cone-Cylinder-Flare and Shock Interaction Analysis [8,12,15,20-22]

Three Dimensional Separated Flow Solutions [6,7,15,19-21]

During the two-year grant period, there have been numerous (26) publications, presentations, dissertations, and other interactions resulting from the research activity. These are listed in Sections (3,5). A review of progress associated with selected research investigations is presented in Section 2. A summary of research highlights, Section 4, concludes the discussion.

2. Progress

2.1 Transient flows in supersonic inlets

In order to demonstrate the effectiveness of the transient RNS formulation for capturing sharp moving shocks, associated shock boundary-layer interaction and unsteady separation, the supersonic flow in two dimensional and axisymmetric inlets, with and without a centerbody, has been evaluated. The main emphasis of these studies has been to accurately predict the transient dynamics of the inlet, vis-a-vis, start and unstart. Inviscid, as well as viscous, laminar and turbulent flow models have been considered. The dynamics of the inlet is greatly influenced by the back pressure, mass bleed and throat area or control mechanism. Changes in back pressure, mass bleed and throat area are typically employed for control

purposes. Although both inviscid and viscous computations capture the qualitative mechanics of start and unstart, the structure of the flow and the quantitative conditions required for start and unstart are significantly influenced by the transient shock boundary-layer interaction.

In all of the computations, the internal and external flow, outside of the cowling, have been coupled and computed simultaneously. The solution for any time step has been obtained using a domain decomposition strategy, where each domain is resolved by a sparse matrix direct solver. The decomposition strategy is devised in such a manner that the computation of the shock is always carried out implicitly, even when the shock is moving across the domain boundaries. This allows for the use of large time steps. For inviscid analysis, in the unstart mode, i.e. for a sufficiently large back pressure, a curved shock stands ahead of the inlet and mass spillage occurs around the cowl. This shock is swallowed by lowering the back pressure or mass bleed. The inviscid computations respond rapidly to small changes in back pressure by moving the shock in and out of the inlet.

For viscous flows the situation is significantly different as the transients depend upon the flow Reynolds number, throat radius and mass bleed. In fact, the inviscid and viscous solutions are contradictory for some flow conditions. An inviscid model may lead to a solution that indicates operation at design conditions with no spillage, while the viscous flow solution, for the same throat area and back pressure, predicts inlet unstart, with mass spillage around the cowl lip. Furthermore, these solutions are greatly influenced by the turbulence model. It should be emphasized that the Reynolds number of the flows considered to date are such that the unsteady flow effects do not influence the transient dynamics of the inlet.

a. Two-dimensional inlet

This is the simplest illustration of inlet dynamics and also simulates the flow in a shock tube, where the reflected shock strongly interacts with

the developing boundary-layer. If the flow is initiated at the unstart solution and the back pressure is then reduced, the shock is swallowed. At the lip of the cowl, a y or lambda shock is formed due to the shock boundary-layer interaction. When the shock is close to the lip of the cowl, it can be expelled by a further increase in the back pressure. This results in the shedding of a vortex which dissipates downstream, see Figs. 1a-b. However, when the shock has moved further into the inlet, further increase in back pressure does not result in moving the shock outside the channel. The size of the reverse flow region depends upon the back pressure. Pressure contours at non-dimensional time 5.52 are depicted in Fig. 1c. An increase in the back pressure somewhat enlarges the recirculation bubble and results in the formation of a 'bulge', where fluid with higher stagnation pressure tends to collect (see Fig. 1c). This phenomena has been observed in a shock tube by M. Herman (NACA TM 1418) who used Schilieren photography, figure 1d.

Any attempt to move the shock out of the channel, e.g., by increasing the back pressure, results in 'divergence' of the solution. Pressure contours and skin friction coefficient just before the solution diverged are shown in Figs. 1e and 1f. This 'divergence' can be eliminated by mass bleed; however, this does not result in an unstart mode. An examination of the solution prior to 'divergence' indicates that breakup of the main recirculating eddy occurs at this point. Further analysis is required to resolve this behavior. This 'divergence' which occurs with both laminar and turbulent models, can be caused by several effects, i.e., (i) the recirculation bubble can not accomodate to the increasing amount of the high stagnation pressure fluid and after some stage bursting occurs, (ii) the eddy breaks up and two or more shedding eddies form, or (iii) a finite time singularity occurs in the equations. For the resolution of this phenomena, these computations must be repeated with much finer spatial grids and decreasing time steps in what amounts to a direct numerical simulation. The

RNS procedure is quite versatile. The code has been adapted to compute flow in multiple inlets. The effect of unstart at one inlet on another is examined. Typical results are depicted in Fig. 1g.

b. Axisymmetric inlet with a centerbody

The general behavior of the axisymmetric flow is similar to that found for the two dimensional inlet and for the case of unstart is depicted in Figs. (2a-b) The shock waves in the axisymmetric case are weaker, and for the same mach number, the y or lambda shock at the lip is weaker and the recirculation region is smaller. Any attempt to unstart the axisymmetric inlet, by increasing the back pressure, resulted in difficulties similar to those encountered in 2D. The restart and unstart of these inlets can be achieved by changing the throat area. As before, a slight reduction of the throat can initiate unstart; however, a large increase in throat area is required for restart. This suggests the existence of a hysteresis phenomena linking the unstart and restart states of the inlet.

c. Effect of bleed

Most of the inlets can be restarted with sufficient mass bleed. This also results in the elimination of the bulge. The second leg of the lambda shock, that was originally straight, now becomes curved. Velocity vectors and pressure contours are depicted in Figs. (2c-d). This leg always terminates at the location where the mass bleed vanishes. Similar phenomena have been observed by Sajben et al experimental results at McDonell-Douglas, see AIAA Pap. No. 90-0379.

d. Diffuser flow

The pressure flux-split solution technique has also been applied for flow in diffusers with inlet swirl. The centrifugal force associated with a swirling velocity component pushes the fluid towards the diffuser wall. As a result, the wall boundary layer is less likely to separate, even if the divergence angle is large and a high pressure recovery coefficient is observed. However, a large amount of swirl reduces the axial velocity near

the centerline, where a reversed flow region is now induced. The flow under such conditions is very complex. The central recirculation region is generally one of a high velocity gradient and intense negative shear. Moreover, there is a significant adverse pressure gradient in the diffuser. These conditions promote flow instability and turbulence production. Analytical solution of such a complex flow field is not possible. Experimental techniques also pose difficulties. Numerical techniques provide a feasible alternate to estimate the flow behavior. However, improved turbulence flow modelling is required. Both the Baldwin-Lomax and the standard k-ϵ model have been applied.

Turbulent flow in a wide angle (45°) diffuser (area ratio of 4) has been computed. The inlet profiles for the axial and swirl velocity are assumed constant. For large swirl velocity a central recirculation region is formed at the center of the diffuser. For these computations a sufficiently fine grid is required close to the surface and centerline. A comparison with results from the teach code is depicted in Fig. 2e. The solutions agree quite well. For the k-ϵ model, the solutions exhibit sensitivity to inflow conditions on both k and ϵ. Two different inflow profiles have resulted in totally different solutions, as seen in the streamline plots (Fig. 2f). For a more accurate prediction, flow conditions obtained from experimental data are required. The effect of grid resolution was examined by considering a fine mesh. A central toroidal recirculation zone is formed near the centerline (Fig. 2g). A forward flow region exists within the recirculation zone. The boundaries of the central recirculation zone on the coarse and fine grids are about the same; however, the coarse grid calculations do not predict the confined forward flow region within the central recirculation zone. Similar toroidal recirculation zones have been observed in experimental studies; however, in many cases, the computational results fail to predict the toroidal nature of the central recirculation zone. This is probably due to the presence of artificial viscosity, and the coarseness of

the grids that are typically used in these calculations. The present study supports the notion that for swirling flows the sensitivity to the turbulent closure model and to the grid is quite severe.

e. Three-dimensional inlet

In the present study, the three-dimensional version of the pressure flux-split scheme has been applied to compute inviscid and viscous flow fields. The scheme is applicable to subsonic, transonic and supersonic flows, and has been extended to high Mach number (Mach > 5) flow fields. The three dimensional scheme also uses flux splitting only along the primary flow direction. The continuity equation is cell centered and the momentum equations in the two cross-plane directions are written at appropriate half points using a trapezoidal or box rule. This maintains second-order accuracy. In the vicinity of an oblique shock, the accuracy of the scheme is lowered by applying pressure-based flux-splitting in the appropriate direction(s).

This formulation has been applied for high Mach number flow in three-dimensional inlets. As a first step, three-dimensional flow along a symmetric corner formed by two intersecting wedges has been examined. Corner flows exist in fuselage wing junctions, in rectangular inlet diffusers and various other aircraft components. Corner flows are characterized by strong three-dimensional viscous-inviscid interactions. In supersonic flow, the flow behavior is further complicated by the presence of shock waves. Inviscid flow at a freestream Mach number of three has been computed. To capture the three dimensional intersecting shock pattern, pressure flux-splitting is appropriately employed in all three directions. Figure 2h depicts the shock pattern at various axial locations. Additional computations at higher Mach numbers and comparison of viscous flow calculations with experimental data will be presented in a future publication.

2.2 Supersonic flow past a cone-cylinder-flare

Axisymmetric laminar flow past a cone-cylinder-flare configuration at $M_\infty = 3$ has been computed. Additional solutions for this configuration of an angle of attack have also been obtained. These are shown in figure 3a. In these calculations, the outer bow shock is fitted and the imbedded recompression shocks are captured. It can be seen that for these flows, with strong viscous/inviscid interaction, the flow behavior and shocks are captured quite well. It should be noted that the RNS global relaxation procedure converges much faster at higher mach numbers. Very recently, additional results for flows over a two-dimensional compression ramp at $M_\infty = 6$, and a variety of Reynolds numbers, have also been obtained for both cold and hot walls. These results are depicted in figures 3(b-c). In these computations, all shocks have been captured. Flow reversal due to shock-boundary-layer interaction in the compression corner is quite evident.

A finite difference implementation of RNS equations, flux-split in each direction, has been applied (Ref. 22) to various compression corner geometries in supersonic flow from Mach 2 to Mach 14. Very good agreement with experimental and other computations has been obtained for attached and recirculating flows. Figure 3d contains a flooded contour plot for Mach 3.0 flow over a 10 degree ramp, showing the overall flow features, and also a comparison of the surface pressure and skin friction with the data of Hung and MacCormack. The separation and reattachment points are accurately predicted. Figure 3e shows the strong shock waves which are captured sharply (about 4 grid points) for Mach 14.1 flow over a 15 degree wedge. Again, excellent agreement of surface pressure and skin friction with experiments of Holden and Moselle and computations of Rudy, Thomas, and Kumar have been obtained.

2.3 Three-dimensional separated flows

Three dimensional computations for laminar flow past afterbody and cone-cylinder-flare configurations of circular, elliptic and hyperelliptic cross-sections have been considered. A semi-coarsening multigrid procedure has been applied to improve the convergence acceleration for three-dimensional flows. At any axial location, the cross-plane solution is obtained by using the sparse matrix solver. In order to reduce the computational cost of the direct solver and allow for fine mesh analysis, advantage is taken of the similarity of the coefficient matrix at neighboring cross-planes. The governing equations are written in delta form and a preconditioner based on the Jacobian, computed at the inflow, is used to drive the residuals to zero. For separated flows, the preconditioner is updated at selected stations. The freezing of the preconditioner leads to the loss of pure quadratic convergence of the Newton iteration. However, it results in a significant savings in the overall computational cost. The use of the multigrid further accelerates the convergence.

Typical results and the convergence acceleration using the multigrid procedure are depicted in Figs. 4(a-c). The extent of the reverse flow region is significantly influenced by the conservation and non-conversation form of the convective terms. On coarse grids, the solutions are in considerable disagreement, however on finer grids these differences are reduced. It is significant that extremely fine meshes are required in order that the separated flow solutions can be considered to be accurate even for engineering purposes. This resolution becomes even more stringent with unsteadiness in the reverse flow regions. Further evaluation is still required. Additional solution on turbulent shock-boundary-layer interaction are depicted in Fig. 4(d-e).

The effect of three-dimensionality on laminar flow breakdown (observed for some two-dimensional configurations) has also been investigated for a trough configuration, with variable aspect ratio. The relief effect,

provided by the three dimensionality, has little influence on the laminar flow behavior that was previously established in the two-dimensional calculations. Further study is required to determine whether this phenomena is problem dependent or whether fine resolution is required in order to resolve this three-dimensional reverse flow interaction.

2.4 Multigrid Domain Decomposition

In order to optimize grid refinement for shock and boundary-layer interactions, adaptive grid generation, and segmental grid refinement, multigrid-domain decomposition strategies have been considered by a number of authors. In most of these investigations, the grid refinement is based on an estimate of the truncation error in the discrete approximation of the governing equations. Since this error includes contributions resulting from the coarseness of the grid, in all independent directions, it is not possible to identify which direction(s) actually need(s) refinement. There is no adaptivity in the directionality of the refinement. In order to resolve a simple boundary-layer, such methods would refine grids in all directions. This is not computationally efficient and would not be appropriate for detailed analysis of shock and separated flow interactions.

A new technique, that allows for an adaptive direction - selective grid refinement, and which insures that the refinement is carried out only in the direction of the sharp gradients, is under investigation. This procedure is made possible by decomposition into multiple domains based on the disparate refinement requirements in different regions. Such a procedure optimally resolves the flow field and, in addition, allows for uniform grids within each domain. The procedure requires appropriate attention to boundary and interface conditions at the various local domain boundaries. The RNS methodology is particularly effective in this regard. With this procedure the appropriate scale lengths are automatically and adaptively prescribed. They agree quite well with the asymptotic theories for the trailing edge

flow and will provide an effective means to analyze local unsteadiness and strong spatial viscous interactions.

In most flow problems, the regions of large gradients constitute a small portion of the flow domain. The adaptive multigrid domain decomposition procedure provides optimal resolution by dynamically identifying the regions of large gradients through a truncation error estimation procedure. Preliminary coarse grid solutions that are relatively inexpensive to compute are used for this purpose. Relevant sections are then refined to form successive multigrid levels. Each multigrid level comprises several subdomains, formed according to the directional refinement requirements. This method provides several advantages in addition to significantly reduces computer resource requirements. It removes any ambiguity relating to the placement of the outflow boundary. It allows for the application of different solvers in different subdomains. This can be significant for very strong interactions. The diffusion terms neglected in the RNS approximation can be included through a deferred corrector after the base RNS solution has been computed. The multigrid transfers play a dual role: 1) information about the outflow boundary location is directed to the fine grid regions, and 2) information is transported back from the fine grid regions to the global (inviscid) coarse grid. This accounts for the viscous-inviscid interaction that is typical of many flows of interest. The use of the RNS system allows for a clear prescription of boundary conditions. There is no need for special interpolation formulae in order to maintain conservation properties (Ref. 23, 24).

For example, in a back step channel flow, the outflow boundary has been placed far downstream and the calculation is still very efficient. The effects of the terms neglected in the RNS approximation can be significant in confined regions of some flow fields. This effect can be captured by including the deferred corrector in appropriate subdomains. Figure 5a shows

the effect, on the backstep channel flow, of including the v_{xx} term as a deferred corrector. Quantitatively, the difference in the solution is not significant, but qualitatively there is a difference. The inclusion of the v_{xx} term leads to a secondary vortex within the primary separation bubble. The local fine grid subdomain allows for the resolution of this secondary recirculation zone.

The non-reflectivity of the outflow boundary condition is another important aspect resulting from the RNS formulation. The calculation for the backstep channel has been performed with the outflow at two different locations, i.e., $x_{max} = 7.0$ and $x_{max} = 15.0$. It is significant that for the $x_{max} = 7.0$ case, the flow is separated at the outflow boundary. Figure 5b shows a comparison of the streamlines obtained from these two computations. Note that there is hardly any difference between the two contour patterns. Figure 5c depicts the streamline contours for the same complex double recirculation (Re=800) flow, only with the outflow boundary at $x_{max} = 30$. These results are in excellent agreement with those of Figure 5b. Figure 5d displays the many grid zones that are obtained for the backstep geometry. Note that the fine grid extent continuously reduces as the flow progresses downstream. Comparison with full NS solutions are excellent (Ref. 25); however, the present formulation requires an order of magnitude less computational time and is started with more severe initial conditions. Figure 5e depicts the grid and trailing edge triple deck structure that is generated with this procedure for the flow past a finite flat plate. Figure 5f shows the excellent comparisons for the severe trailing edge pressure gradient. These trailing edge calculations, with large numbers of mesh points placed appropriately, are computationally inexpensive, e.g. 1 to 2 minutes on an IBM workstation. This procedure has now been established as a

valuable tool for future analysis of high frequency flow behavior and strong viscous interaction.

3. Interactions

During the period of this annual report there have been interactions with several outside researchers; in addition, one Ph.D graduate, Dr. T. Liang has accepted employment with the GE Aircraft Engines, CFD branch. Dr. Eric Bender, at General Dynamics, is continuing his investigation on the application of RNS direct solver procedures for chemically reacting flows. A paper was presented at the 1990 AIAA Fluids meeting in Seattle. There were also many fruitful discussions concerning a possible joint effort. The PI's have had extensive discussions with Drs. Luke Schutzenhofer, Helen McConnaughy and Kevin Tucker regarding code validation for application to flows in engine geometries.

RNS procedures for internal flows are under investigation at the NASA Lewis Research Center by T. Bensen, J. Adamcyzk, and by D.R. Reddy at Sverdrup, a Lewis contractor. A number of meetings have taken place with these researchers. A seminar was given by one of the PI's (SGR) at Sverdrup. Several related papers on supersonic inlet unstart/restart have either appeared or have been submitted for publication. Applications to turbomachinery are also being considered.

Several researchers from NASA Lewis, WPAFB and AFIT have developed interest in the composite and RNS techniques. Mark Celestina of Sverdrup and Philip Morgan from WPAFB have initiated studies in our Ph.D program. Mary Brown originally from Elgin AFB, has started MS work on applications to supersonic blunt bodies. Prof. C. Fletcher of the University of Sydney has devoted a complete chapter on RNS techniques and solutions in a recent book on computational fluid dynamics. One of the PIs (SGR) and Dr. John Tannehill of Iowa State University have been invited to provide an article on "PNS/RNS Computational Methodology" for the 1992 Volume of Annual Review in Fluid Mechanics.

Roger Cohen who spent two years at the University of Cincinnati as a Fulbright fellow, is currently finishing his Ph.D under the supervision of Prof. Fletcher at the University of Sydney in Australia. He has presented two recent papers on RNS direct solver solutions at the International CFD Conferences in Brisbane and Tokyo. Roger is also investigating other re-ordering techniques and the application of conjugate gradient methods to further enhance the RNS direct solver approach.

Dr.'s H.C. Raven and M. Hoekstra of the Maritime Research Institute in Netherlands are also continuing the successful application of RNS techniques to the solutions for hydrodynamic (ship) computations. Recently they presented their work at a ship hydrodynamics workshop in Sweden. Prof. A. Roberts and his associate at the University of Glasgow have also expressed considerable interest in the RNS solution methodology for high speed flows. They have recently presented PNS computations at the 12th INCFM Conference at Oxford University and very interesting discussions were initiated to extend their calculations for viscous interactions where RNS methods are required. For high mach number supersonic and hypersonic flows, the RNS formulation is also being considered by several investigators at UTRC and by Dr. D.R. Reddy of Sverdrup.

4. Highlights of Research Progress

(a) For transient flows in supersonic inlets, it has been found that shock-boundary-layer interaction significantly influences the processes of unstart and restart. With an increase in back pressure, it is found that high stagnation pressure fluid tends to collect within the recirculation eddy near the foot of the lambda shock. This eddy has a tendency to break into multiple zones. The inlet can be restarted with sufficient mass bleed. It is found that the lambda shock always terminates precisely where the bleed vanishes. A similar phenomenon has been observed in Sajben's experiments at McDonell Douglas. A small reduction in throat area can also initiate unstart; however, it has

been shown that a much larger increase in throat area is required for restart. This suggests the existence of a hysteresis curve connecting the start and unstart limits.

(b) The prediction of laminar flow breakdown in a three-dimensional trough with spanwise variation of depth, suggests that transition within the recirculation region first initiates near the symmetry plane. This result is clearly problem dependent and further analysis is required.

(c) Three-dimensional separated flows for subsonic and supersonic freestream conditions have been computed with both laminar and turbulent models. Artificial viscosity is not required for these computations.

(d) Adaptive and fixed domain decomposition strategies for fine mesh evaluation of strongly interacting flows have been developed. When combined with a direct solver, for subdomain with large transients or strong viscous interactions, this procedure leads to an efficient and robust solution algorithm. Flows with moving shocks, recirculation regions, lambda shocks have been computed by this technique.

(f) The pressure-split flux vector procedure has now been extended to arbitrary non-orthogonal coordinates and to regions where the main flow direction is not locally along the surface or in the primary flow direction, e.g. blunt body flows. The role of the RNS boundary conditions in the formulation of the difference approximations has also been clarified.

5. AFOSR Publications, Presentations, Related Activity and Interaction 12/89-11/91

A. Publications and Proceedings

1. Rosenbaum, D. and Rubin S.G., "Global Pressure Relaxation for Laminar 2-D Internal Flow", Int. J. for Numerical Methods in Fluids, 10, pp. 827-48, June 1990.

2. Pordal, H.S., Khosla, P.K. and Rubin, S.G., "Inviscid Steady/Unsteady Flow Calculations," Computers & Fluids, 19, pp. 93-118, January 1991.

3. Pordal, H.S., Khosla, P.K. and Rubin, S.G., "A Flux Split Procedure for Calculations," Proc. of the ASME/CSME Int. Conf. on Unsteady Flows, Toronto, June 1990.

4. Pordal, H.S., Khosla, P.K. and Rubin, S.G., "Unsteady Viscous and Inviscid Supersonic Flow Calculations in Axisymmetric Inlets," 28th Aerospace Sciences Meeting, AIAA Paper No. 90-0585, Reno, 1990.

5. Pordal, H.S., Khosla, P.K. and Rubin, S.G., "Supersonic Turbulent Flows in Inlets," Proceedings CFD Symposium on Aeropropulsion, NASA CP 10045, Cleveland, 1990.

6. Almahroos, H., Khosla, P.K. and Rubin, S.G., "Subsonic/Transonic Flow Calculations Over 3-D Afterbodies," Proceedings Symposium on Aeropropulsion, NASA CP 10045, Cleveland, 1990.

7. Gordnier, R.E. and Rubin, S.G.: Three Dimensional Composite Velocity Solutions for Subsonic/Transonic Flow Over Afterbodies, accepted for AIAA Journal, 29, 5, pp. 750-57, May 1991.

8. Rubin, S.G. and Khosla, P.K., "A Review of Reduced Navier-Stokes Computations for Compressible Viscous Flows", J. Comp. Syst. in Eng., 1, pp. 549-562, 1990.

9. Pordal, H.S., Khosla, P.K. and Rubin, S.G., "A Flux Split Procedure for Calculations", accepted to the Journal of Fluids Engineering.

10. Pordal, H.S., Khosla, P.K. and Rubin, S.G., "Transient Behavior of Supersonic Flow Through Inlets", accepted to AIAA Journal.

B. Presentations, Seminars and Other Student Activity

11. Pordal, H.S., Khosla, P.K. and Rubin, S.G., "Transient Behavior of Supersonic Flow Through Inlets", AIAA Paper No. 90-2130, Presented at 26th Joint Propulsion Conference, Orlando, FL., 1990.

12. Khosla, P.K., Liang, T.E. and Rubin, S.G., "Supersonic Viscous Flow Calculations for Axisymmetric Configurations", Presented at 12th International Conference on Computational Fluid Dynamics, Oxford, England, July 1990.

13. Himansu, A. and Rubin, S.G., "Three-Dimensional RNS Computations with Multigrid Acceleration", AIAA Paper No. 91-0105, 29th Aerospace Sciences Meeting, Reno, 1991.

14. Pordal, H.S., Khosla, P.K. and Rubin, S.G., "Pressure Flux Split Reduced Navier-Stokes Solutions for Subsonic Diffusers", AIAA 22nd Fluid and Plasma Dynamics Meeting, AIAA Paper No. 91-1745, Honolulu, HA., 1991.

15. Khosla, P.K., Liang, T.E. and Rubin, S.G., "Supersonic Viscous Flow Calculations for Axisymmetric and Three-Dimensional Configurations", AIAA 22nd Fluid and Plasma Dynamics Meeting, AIAA Paper No. 91-1802, Honolulu, HA., 1991.

16. Khosla, P.K. and Rubin, S.G., "Pressure Based Flux Vector Splitting for Blunt Geometries", Proceedings 10th AIAA Computational Fluid Dynamics Meeting, Honolulu, HA., pp. 975-76, 1991.

17. Rubin, S.G., Seminar "RNS Methodology for Transient and Recirculating Flows", Sverdrup Corporation, Cleveland, Ohio, 1990.

18. Khosla, P.K. and Rubin, S.G. (Invited), "Pressure-Based Procedure for Shock-Boundary Layer Interaction", Proceedings 4th International Symposium on Computational Fluid Dynamics, University of California, Davis, CA., 1991.

19. Rubin, S.G., Almahroos, H.M.H. and Khosla, P.K. (Invited), "Viscous Inviscid Interactions for 3D Afterbody Flow, Proceedings 4th International Symposium on CFD, Davis, CA., pp. 987-92, 1991.

20. Rubin, S.G. and Tannehill, J., "PNS/RNS Computational Techniques", Annual Review of Fluid Mechanics, pp. 117-44, 1992.

21. Som, A., M.S. Thesis, "Supersonic Flow Past a Cone-Cylinder Flare Configuration", University of Cincinnati, 1990.

22. Hagenmaier, M., M.S. Thesis, "Supersonic Flow Along a Compression Corner", University of Cincinnati, 1991.

23. Srinivasan, K., M.S. Thesis, "Multigrid Domain Decomposition for Viscous Interacting Flows", 1991.

24. Srinivasan, K. and Rubin, S.G., "Adaptive Multigrid Domain Decomposition for RNS Equations", Proceedings 5th SIAM Conferences on Domain Decomposition Methods, Norfolk, VA., 1991

25. Rubin, S.G. and Srinivasan, K. (Invited), "A Multigrid Domain Decomposition Strategy for Viscous Flow Calculations", Proceedings 5th Symposium on Numerical and Physical Aspects of Aerodynamic Flows, Long Beach, CA., 1992.

26. Pordal, H., "Supersonic Inlet flows", Ph.D Dissertation, University of Cincinnati, 1991.

C. Committees and Assignments

S.G. Rubin (1989-91):

Member of the Advisory Committee for Institute for Computational Methods in Propulsion (ICOMP) (Case Institute/NASA Lewis)

Consultant to the NASA (OAST) Aerospace Research and Technology Subcommittee (ARTS) of the Aeronautics Advisory Committee (AAC)

Collatoral Faculty Member, Ohio Aerospace Institute

Editor-in-Chief, Int'l Journal, Computers and Fluids, Pergamon Press

Session Chairman, 12th AIAA CFD Conference, Honolulu, 1991

Invited Speaker, 3rd CFD Aerodynamics Conference, Washington, D.C., 1990

Member, SAE Condition Monitoring Technical Committee

Invited Speaker (with P.K. Khosla), 4th Int'l conference on CFD, Davis, CA., 1991

P.K. Khosla (1991):

Member of Editorial Advisory Board, Int'l Journal, Computers and Fluids

Collatoral Faculty Member, Ohio Aerospace Institute

D. Students Supported (1989-91)

1.	H. Pordal, M.S. 1986, Ph.D 1991	
2.	A. Himansu	Ph.D expected 1992
3.	Mark Hagenmaier, M.S. 1991	Qualified Ph.D Student
4.	A. Som, M.S. 1991	
5.	Mary Brown	M.S. Student
6.	Phil Morgan	Ph.D Student
7.	H. Almahroos	Qualified Ph.D Student
8.	David Brown, M.S. 1991	Ph.D Student
9.	K. Srinivasan, M.S. 1991	Qualified Ph.D Student

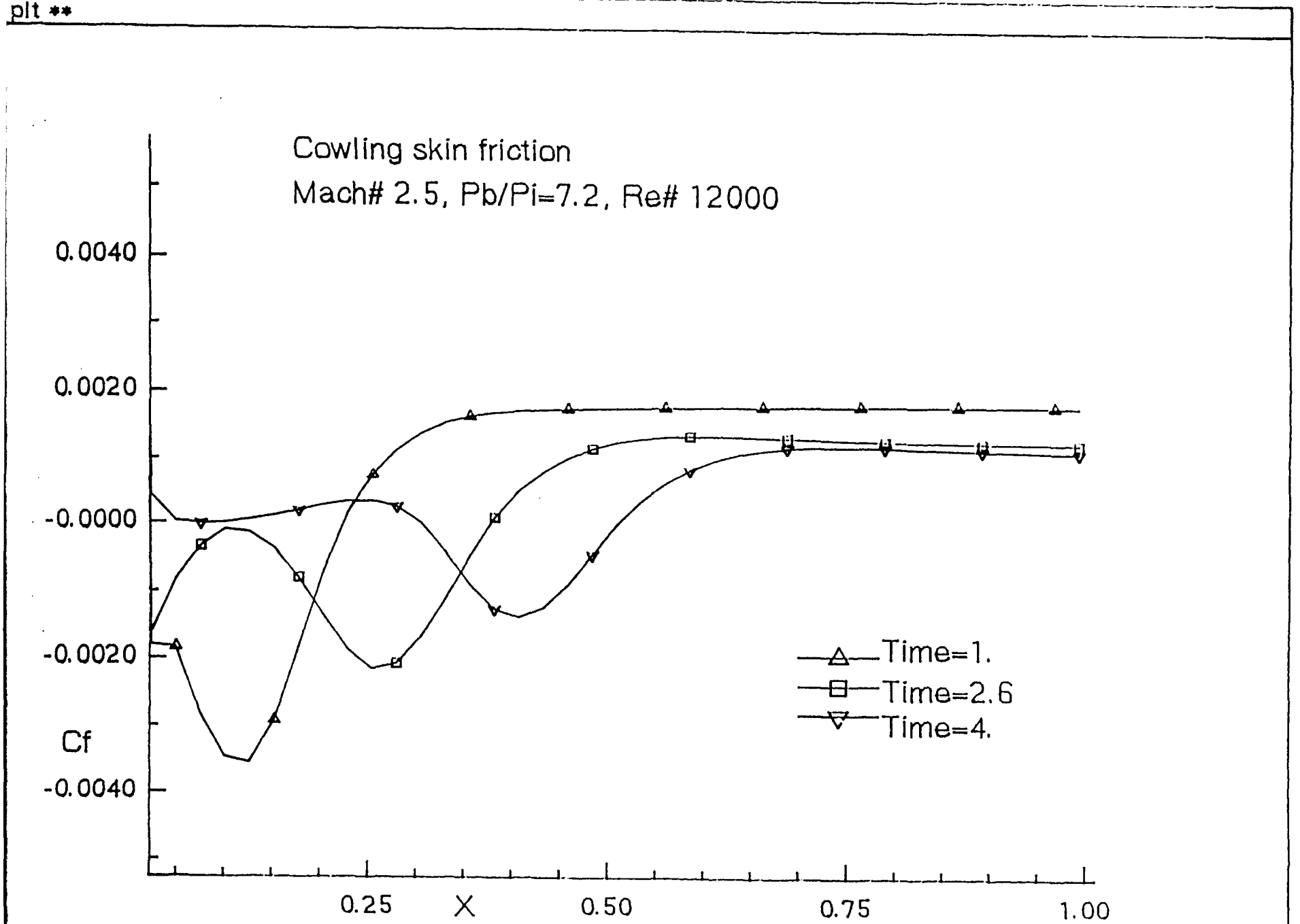

Figure 1a. Vortex shedding during unstart of the inlet

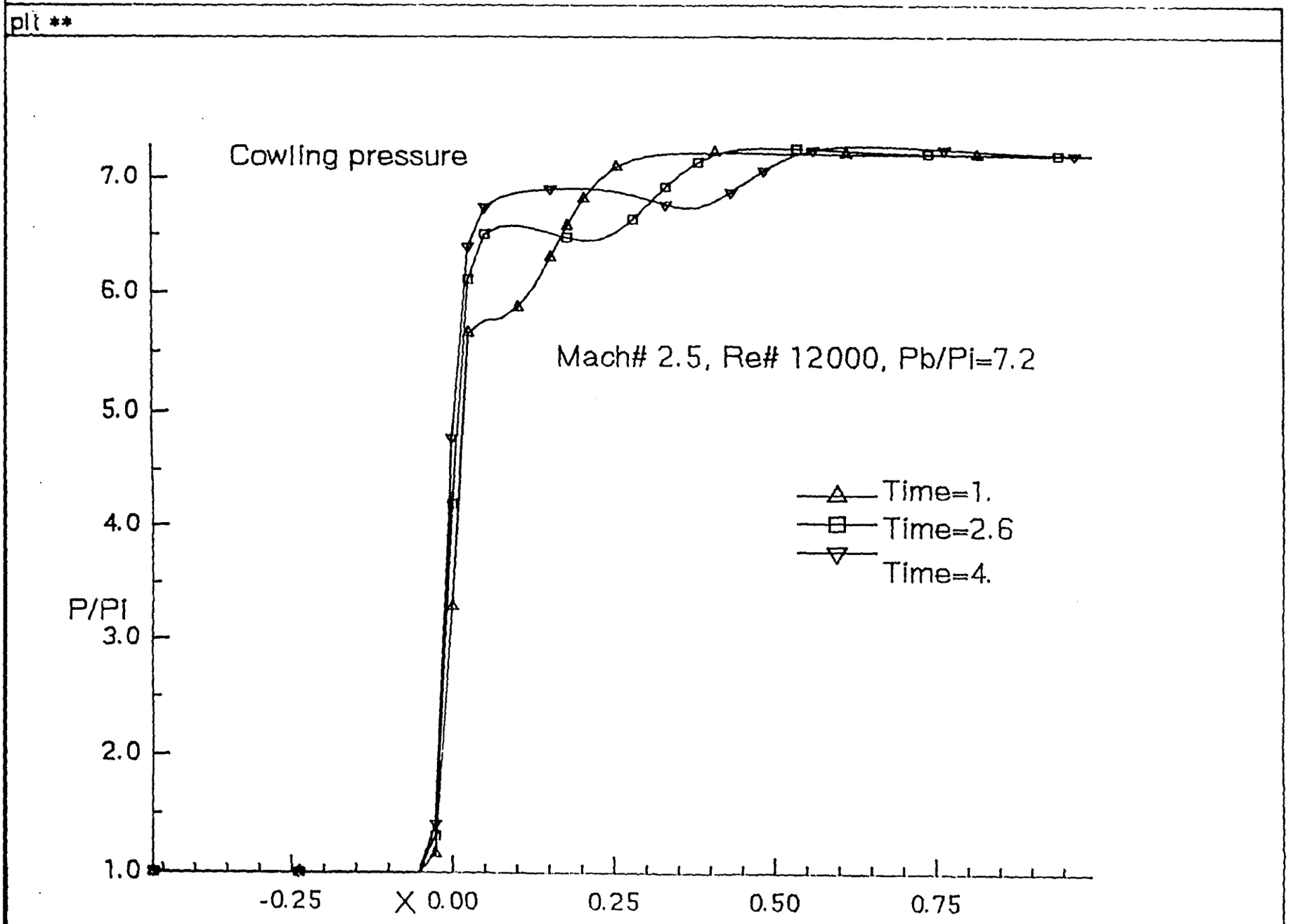

Figure 1b. Pressure distribution during vortex shedding

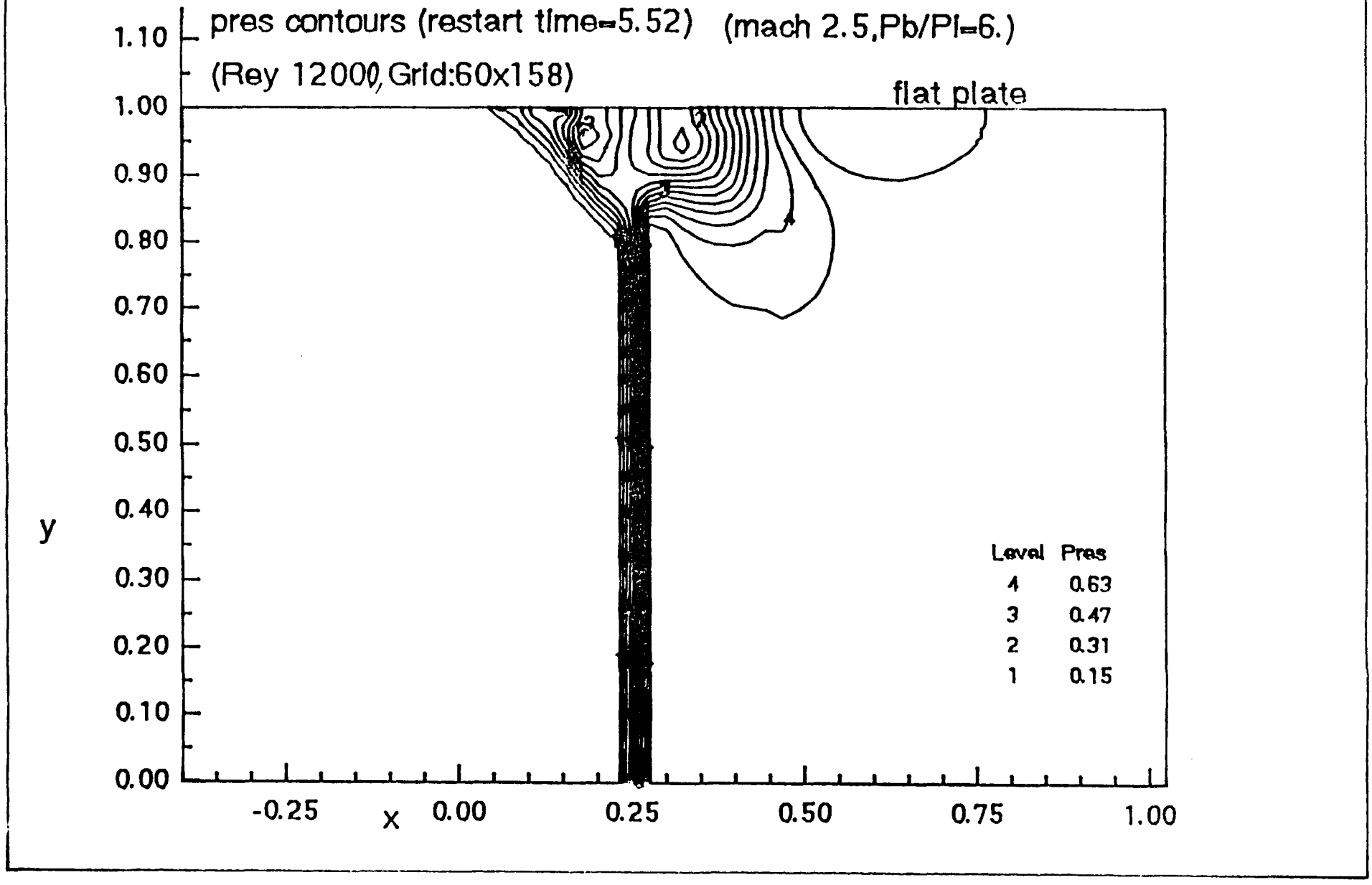

Figure 1c. Lambda shock in an inlet

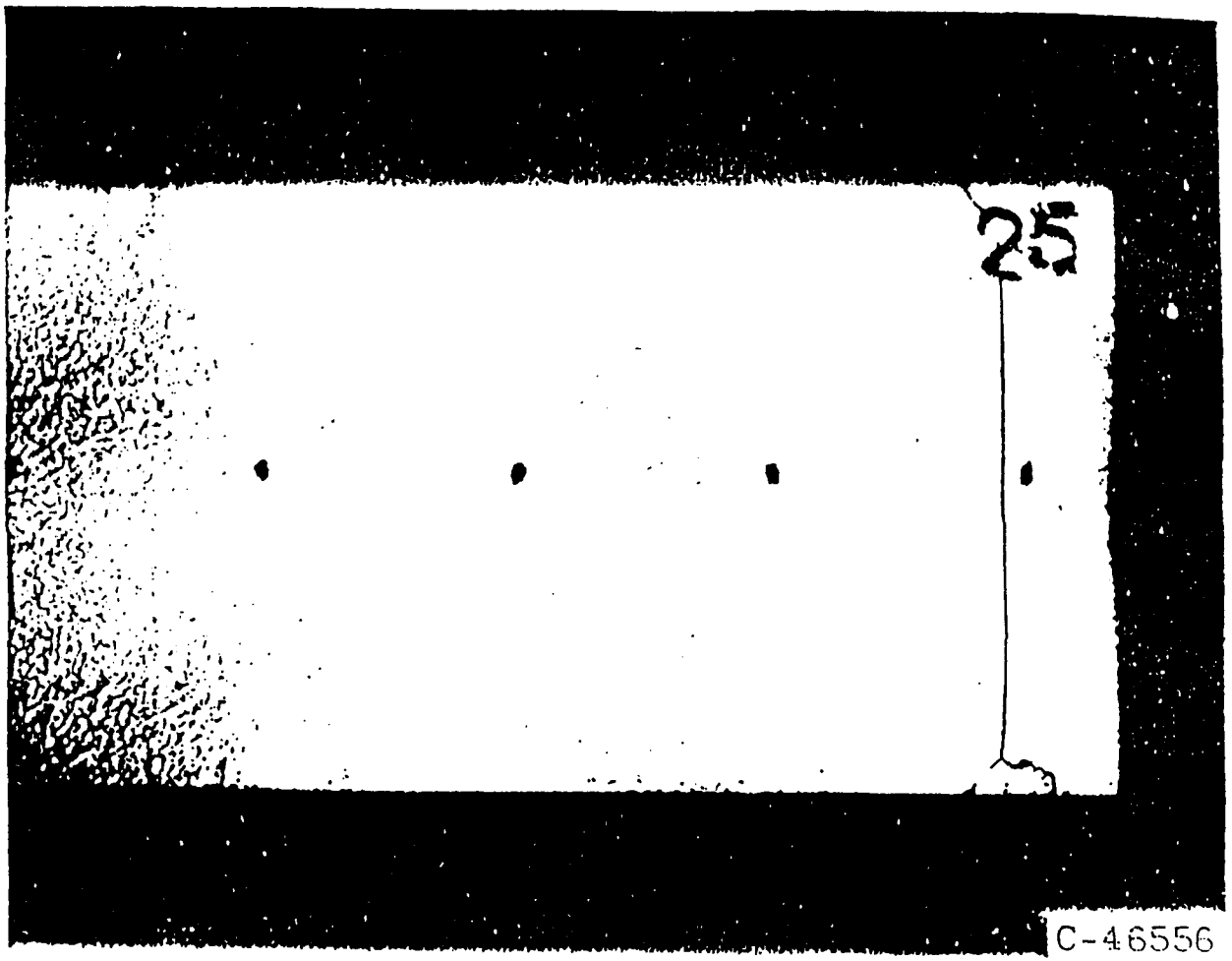

Figure 1d. Lambda shock in shock tube experiment (M. Herman)

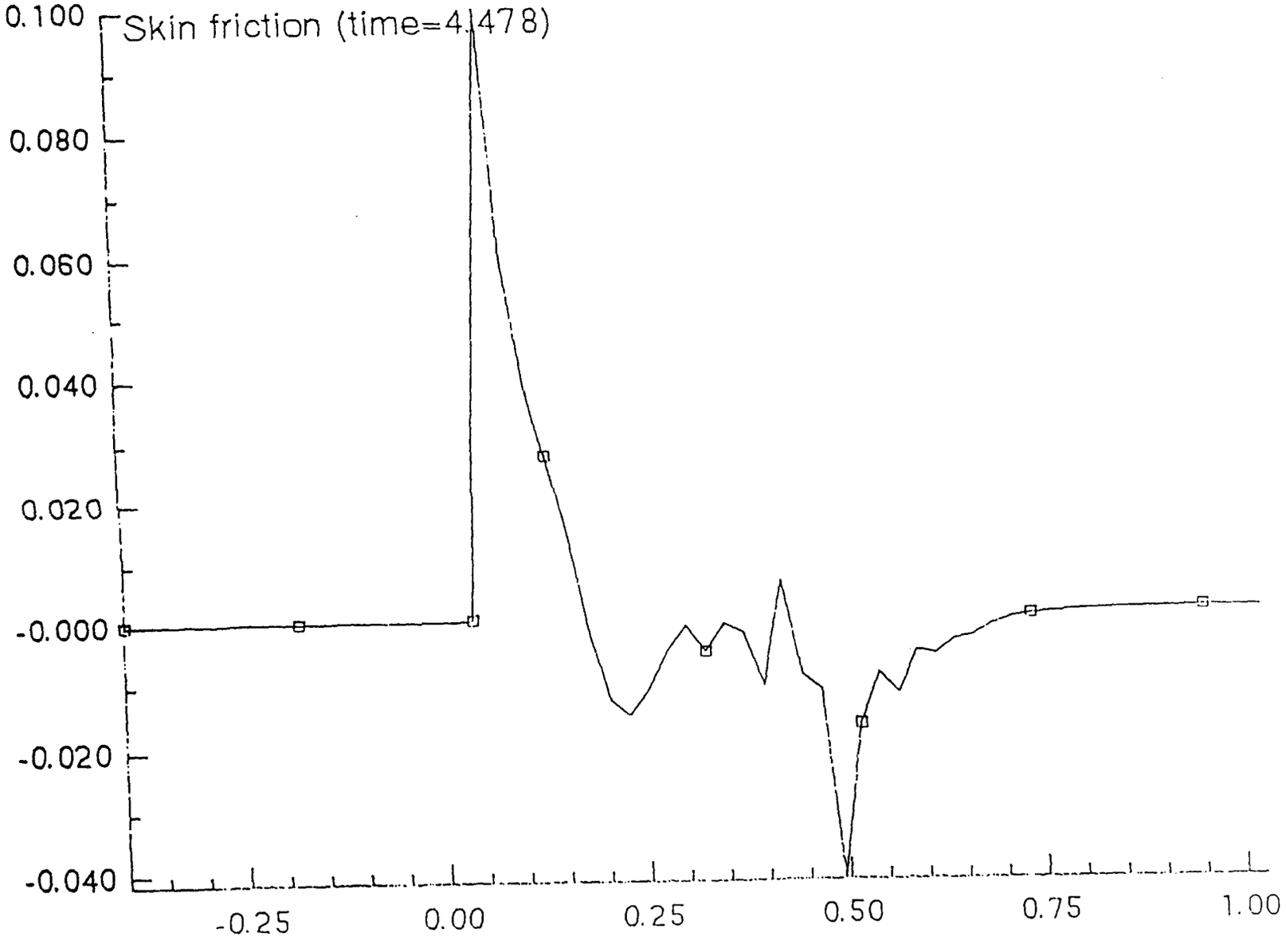

Figure 1e. Vortex breakup due to shock boundary-layer interaction

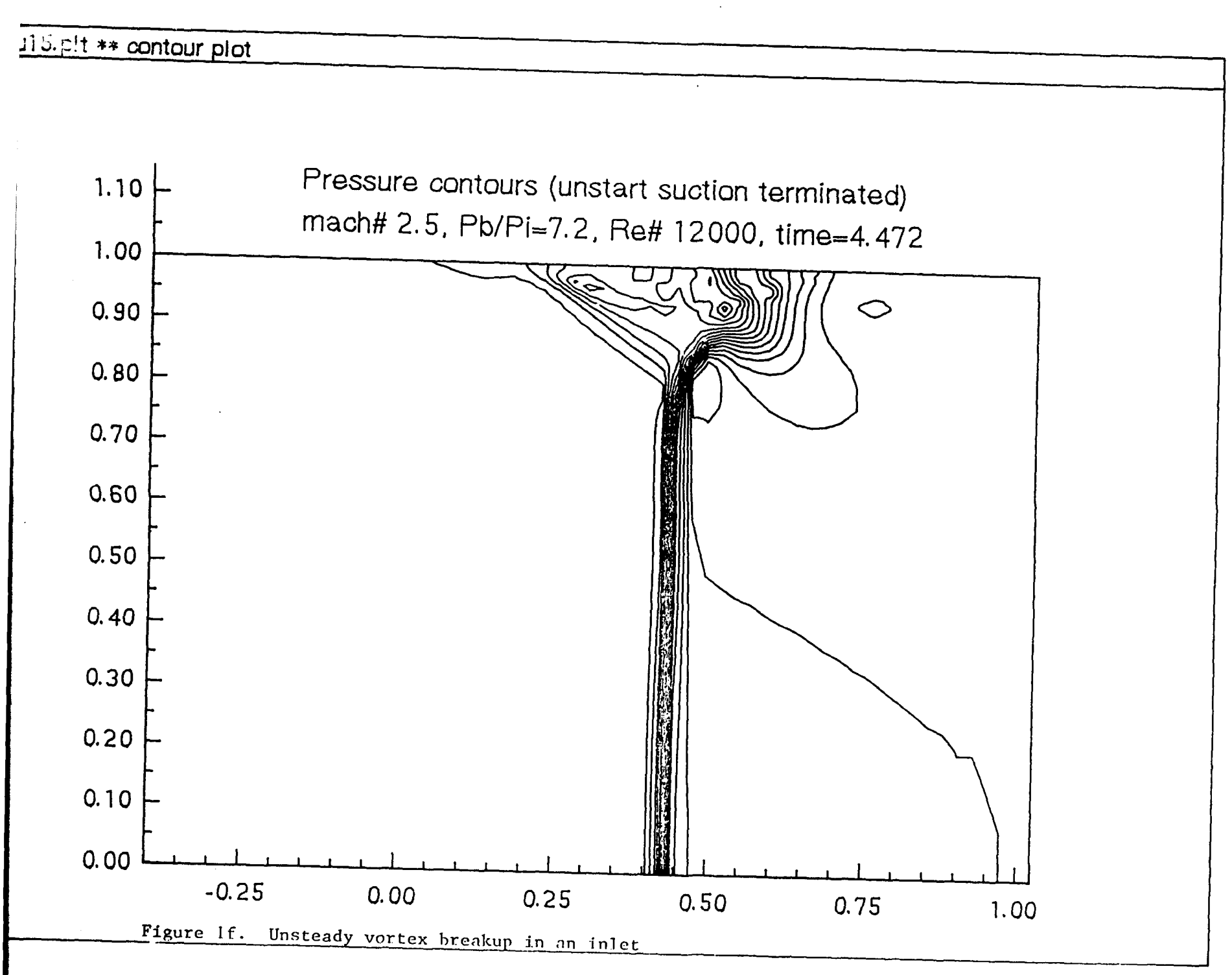

Figure 1f. Unsteady vortex breakup in an inlet

FIG. 19 MULTIPLE INLET INTERACTIONS WITH SHOCKS

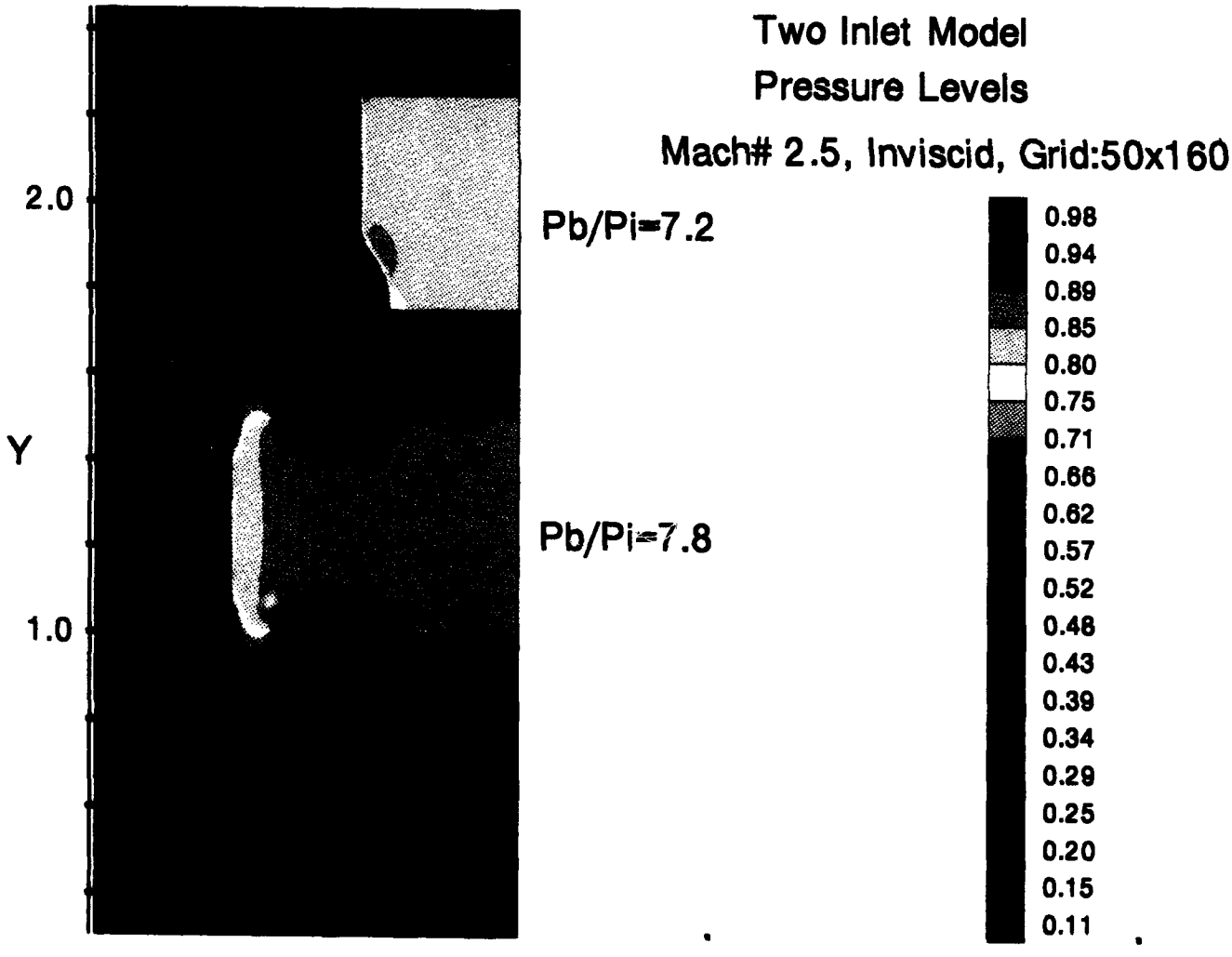

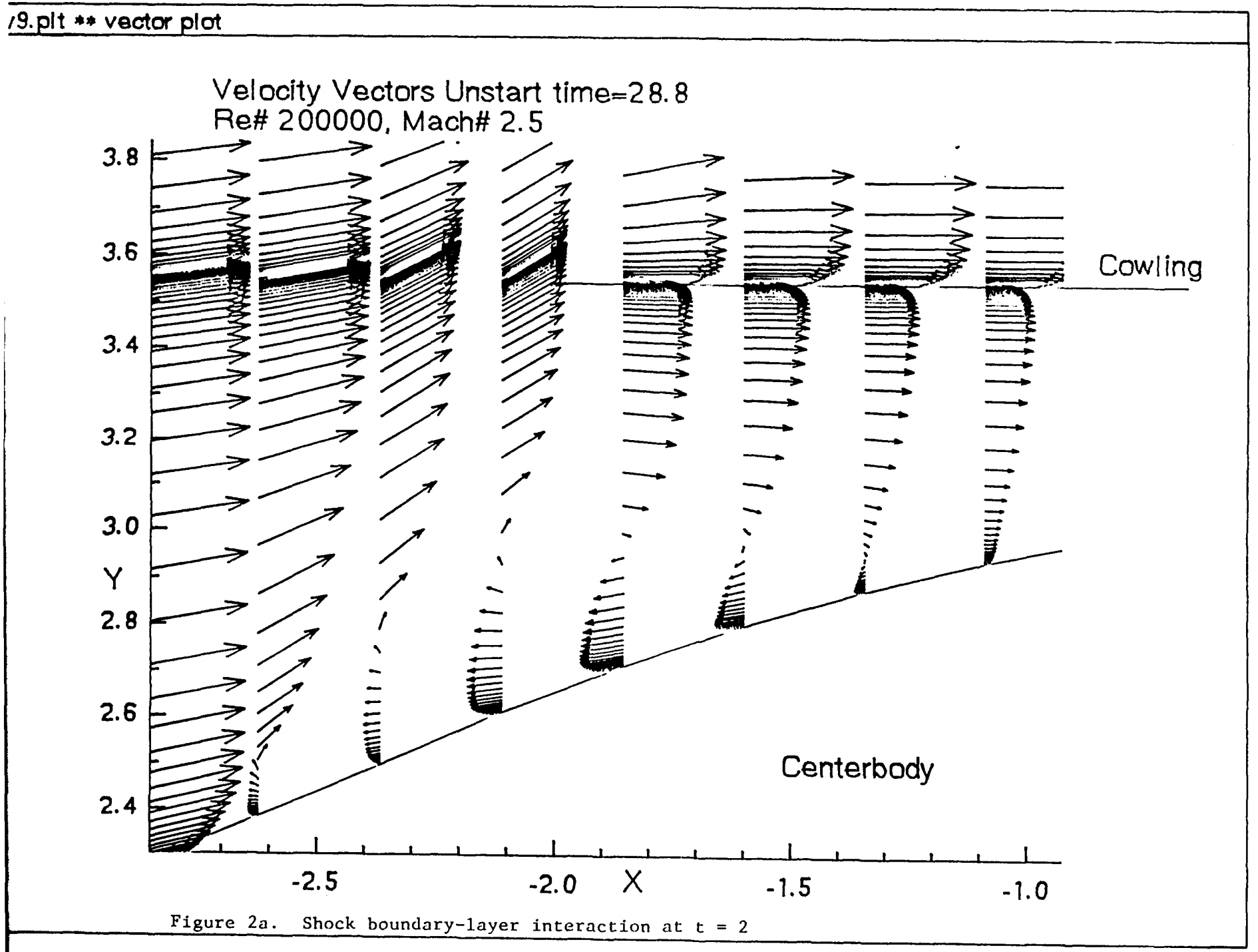

Figure 2a. Shock boundary-layer interaction at t = 2

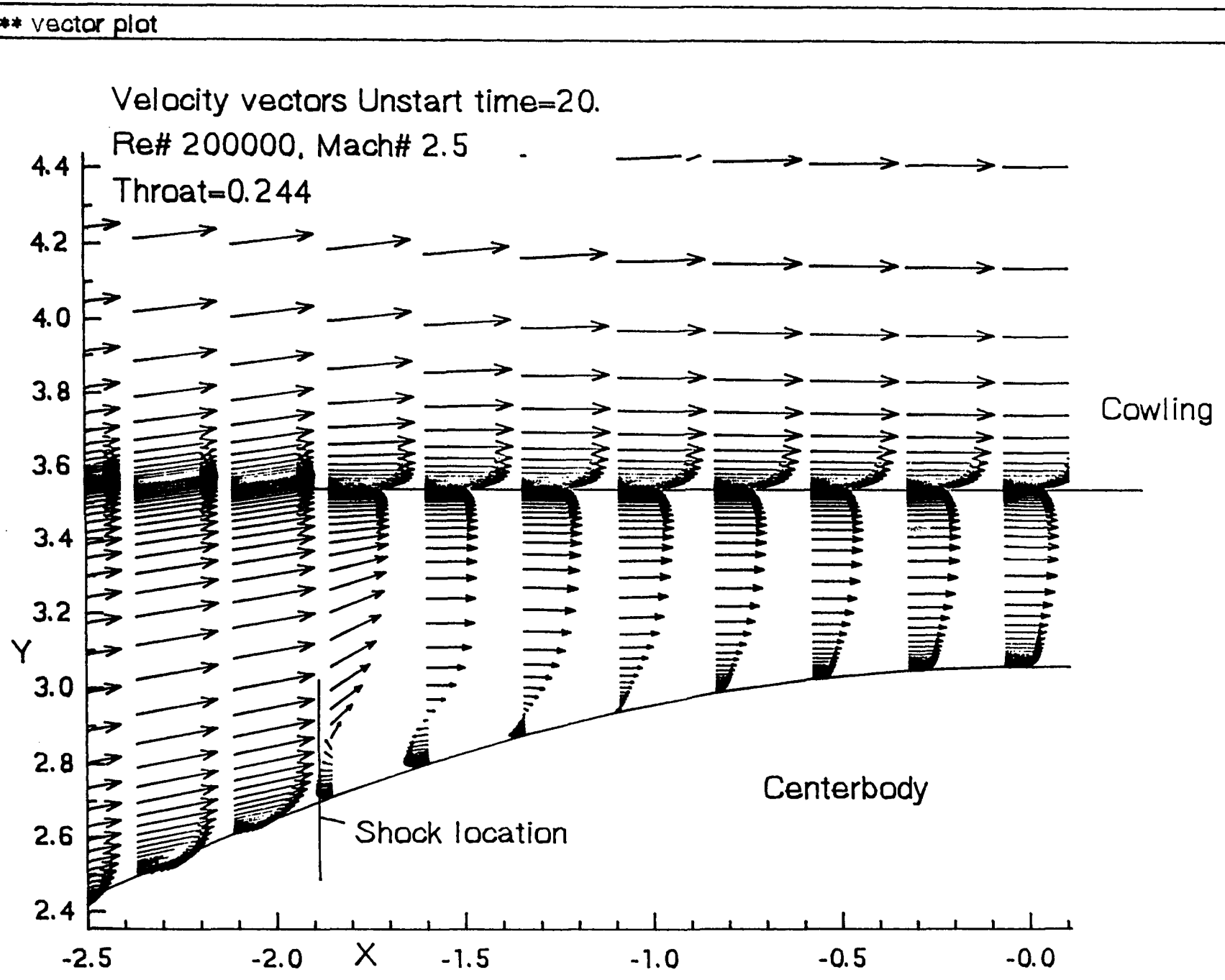

Figure 2b. Shock boundary-layer interaction at t = 28.8

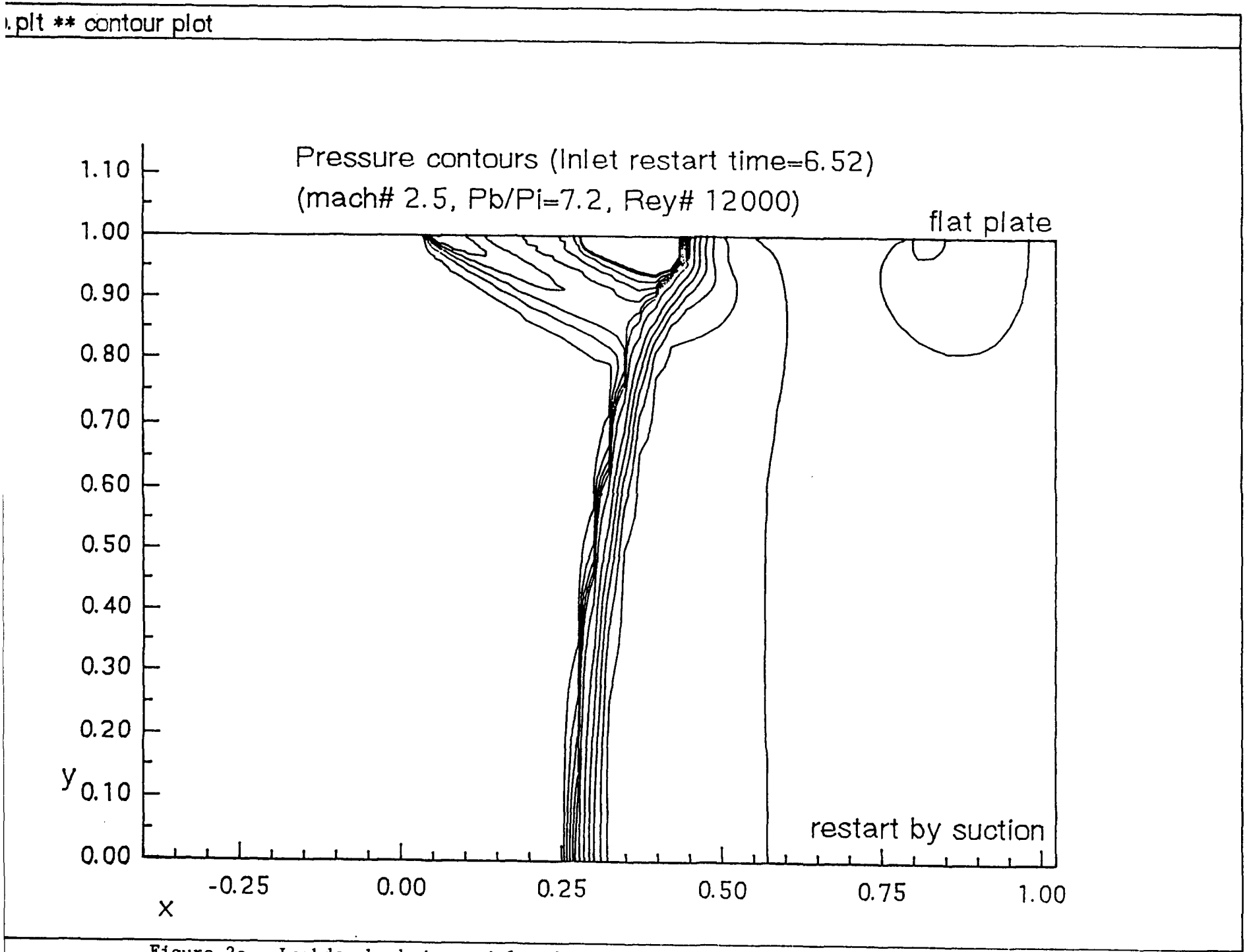

Figure 2c. Lambda shock in an inlet due to bleed

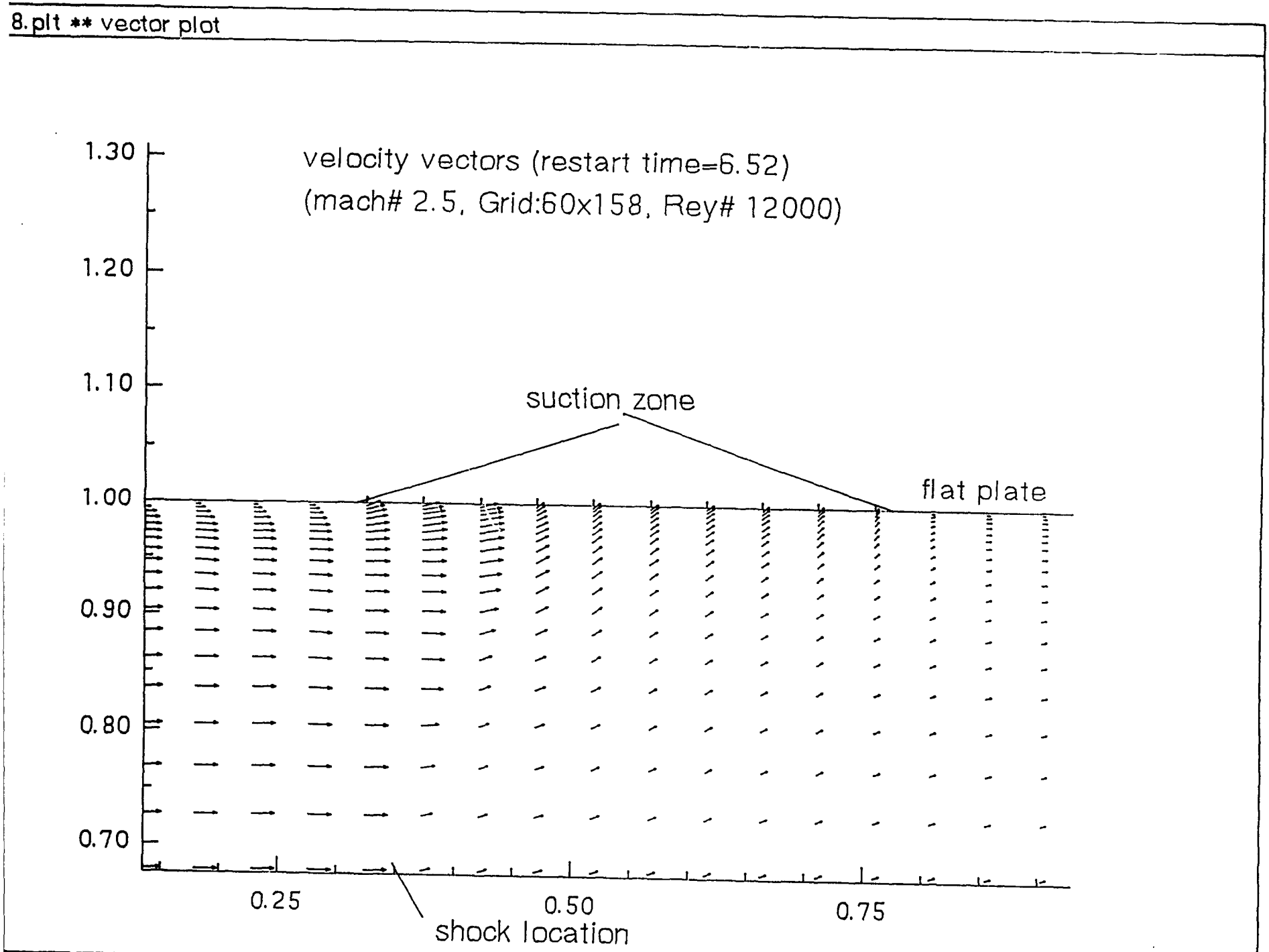

Figure 2d. Shock-boundary-layer interaction in the bleed zone

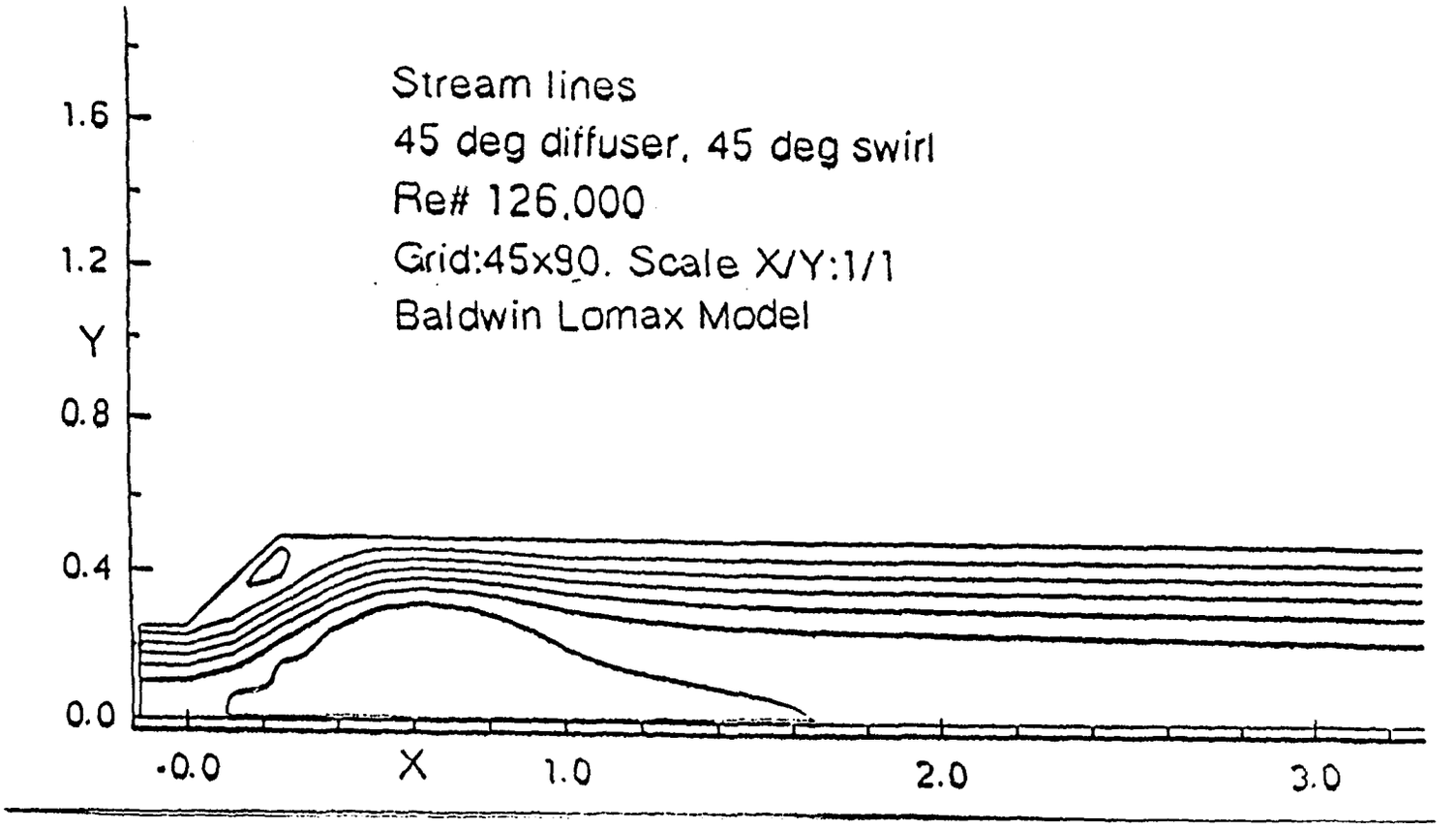

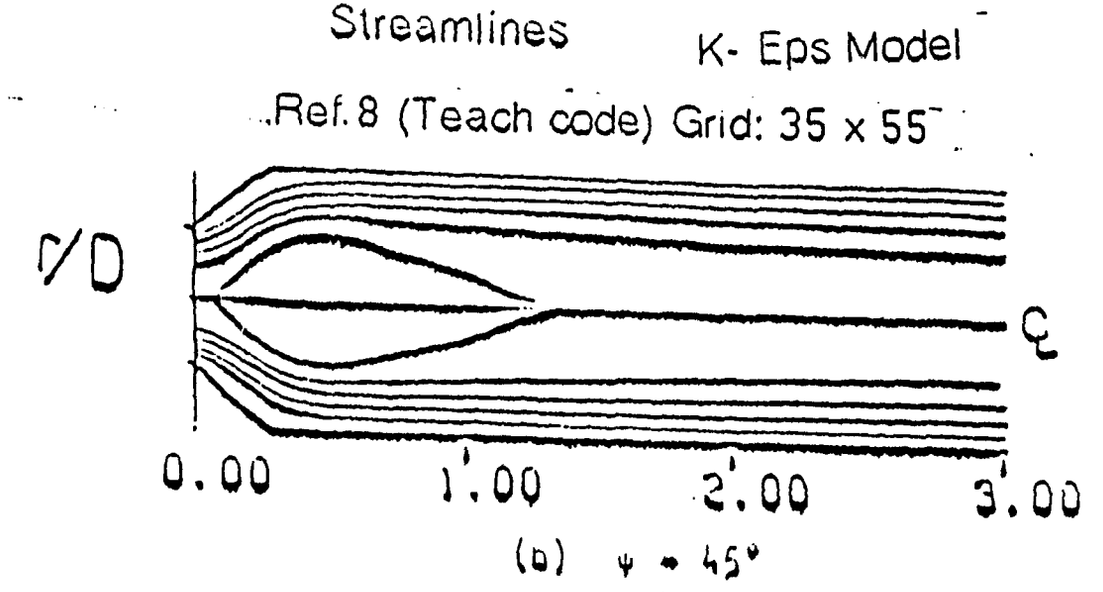

FIG. 2e DIFFUSER STREAMLINES

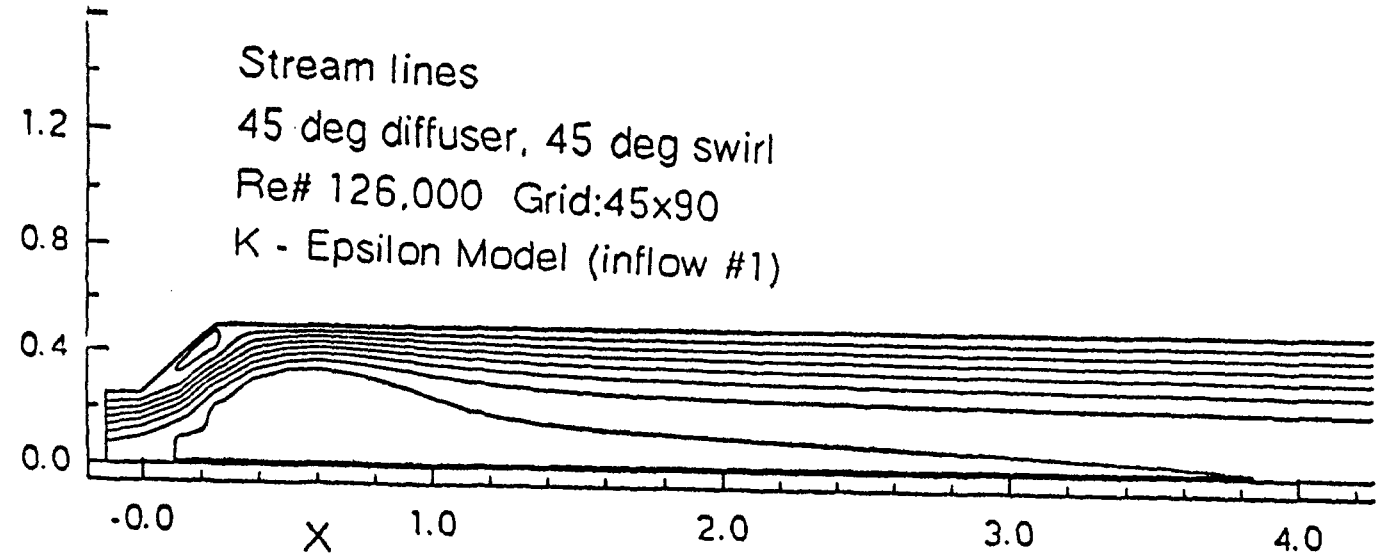

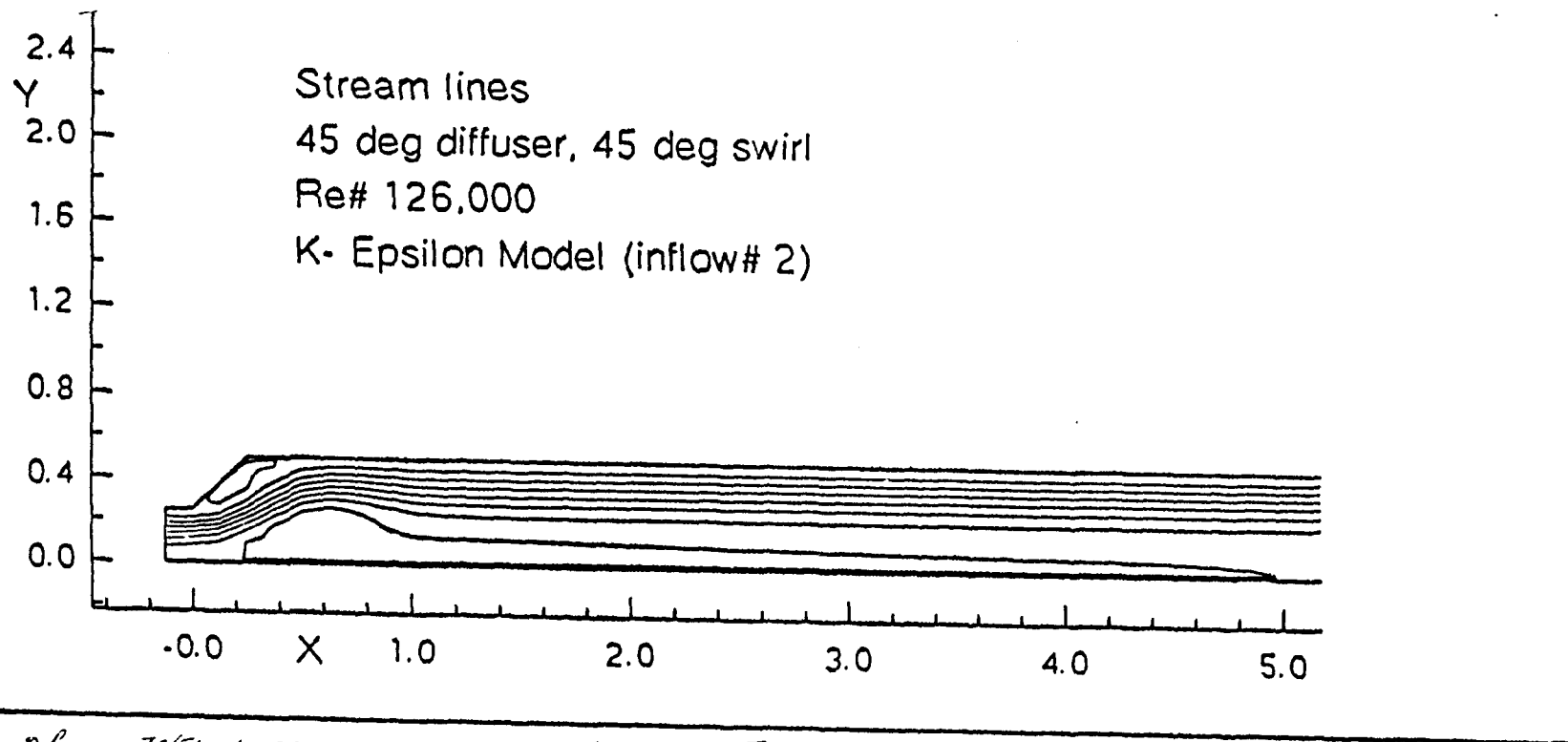

FIG. 2f INFLOW PROFILE EFFECTS ON DIFFUSER FLOW

Fig 29 Grid Studies for Diffuser Flow

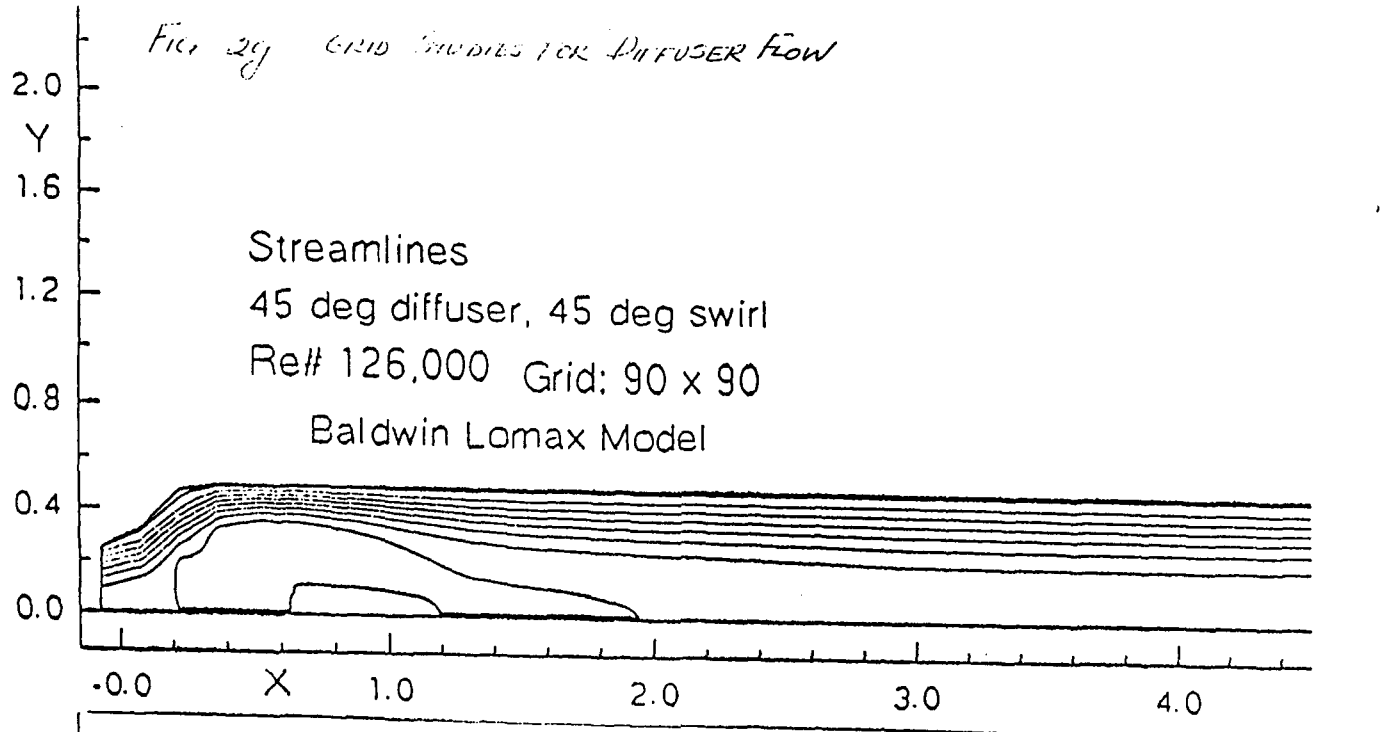

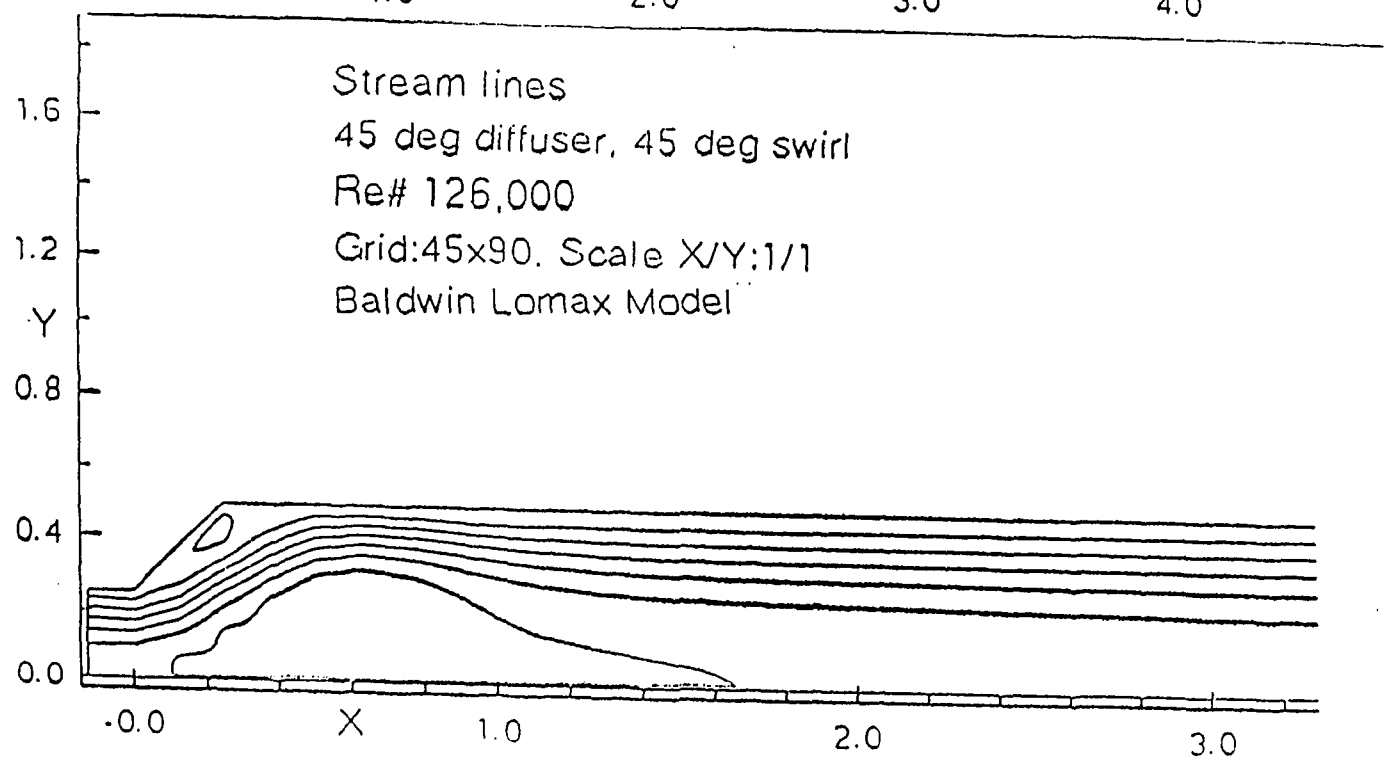

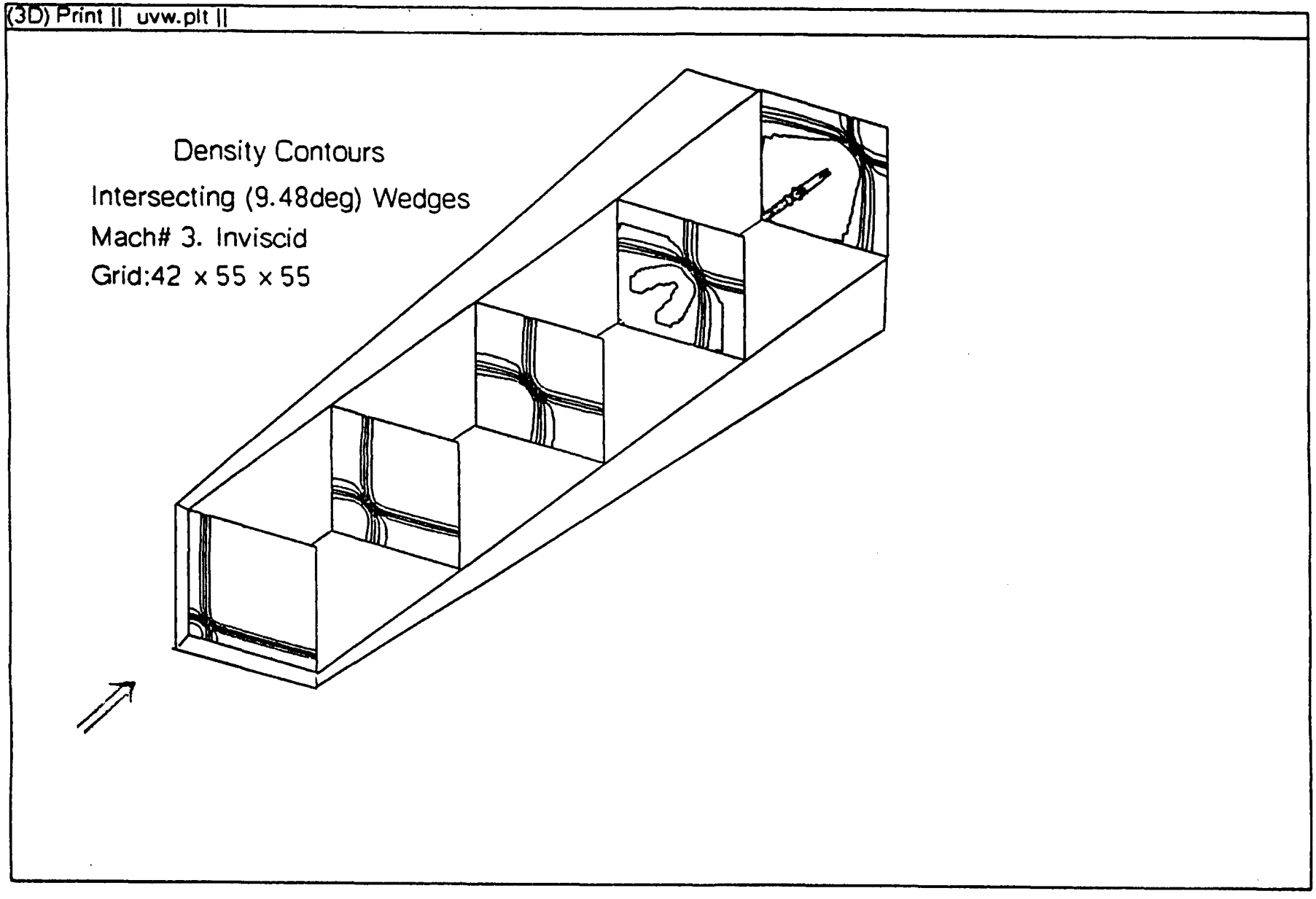

FIG 2h : SHOCK PATTERNS FOR A RECTANGULAR INLET

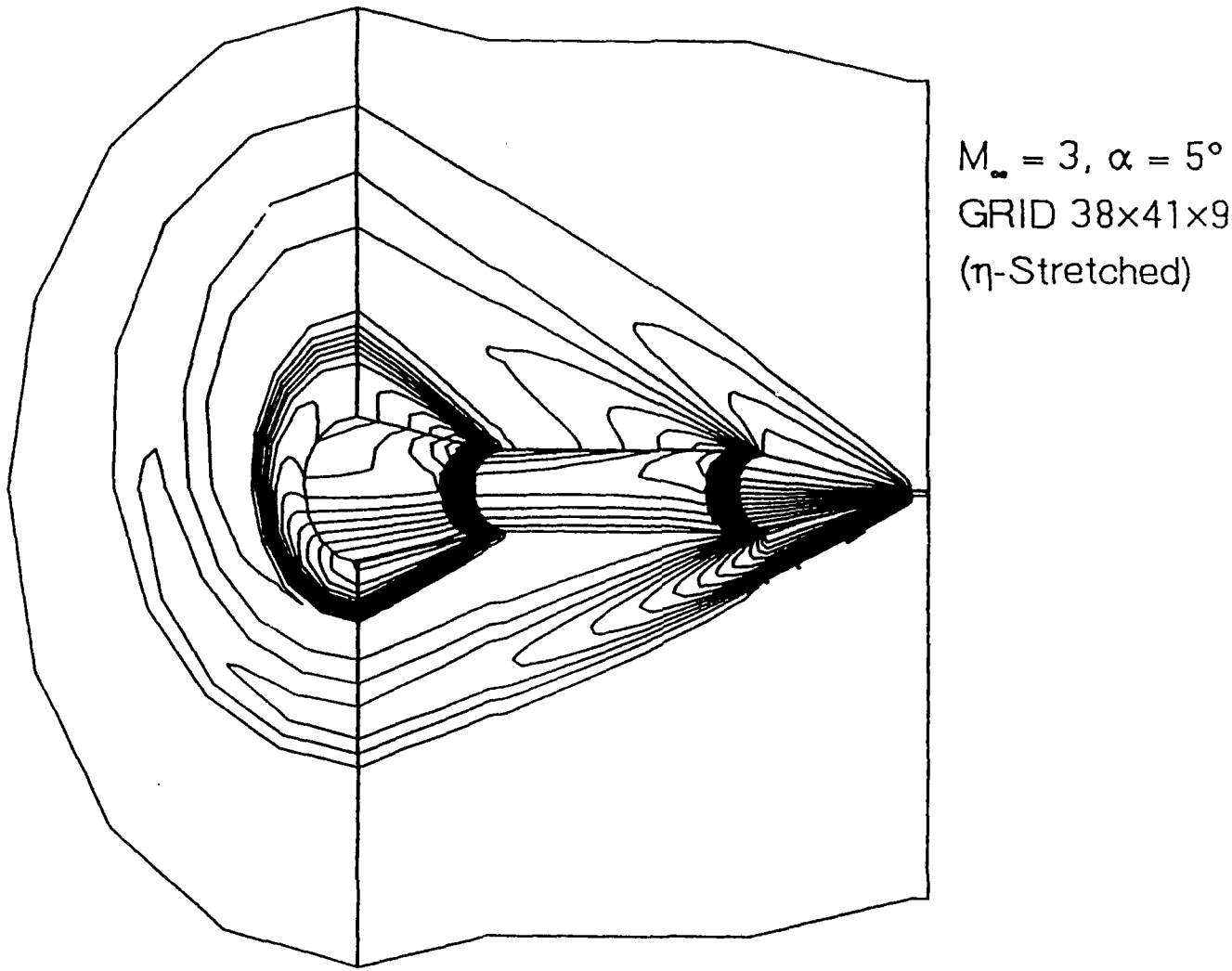

Figure 3a. Cone-Cylinder-10°Flare, M_∞=3, α=5°, (38×41×9): Three dimensional view of C_p contours.

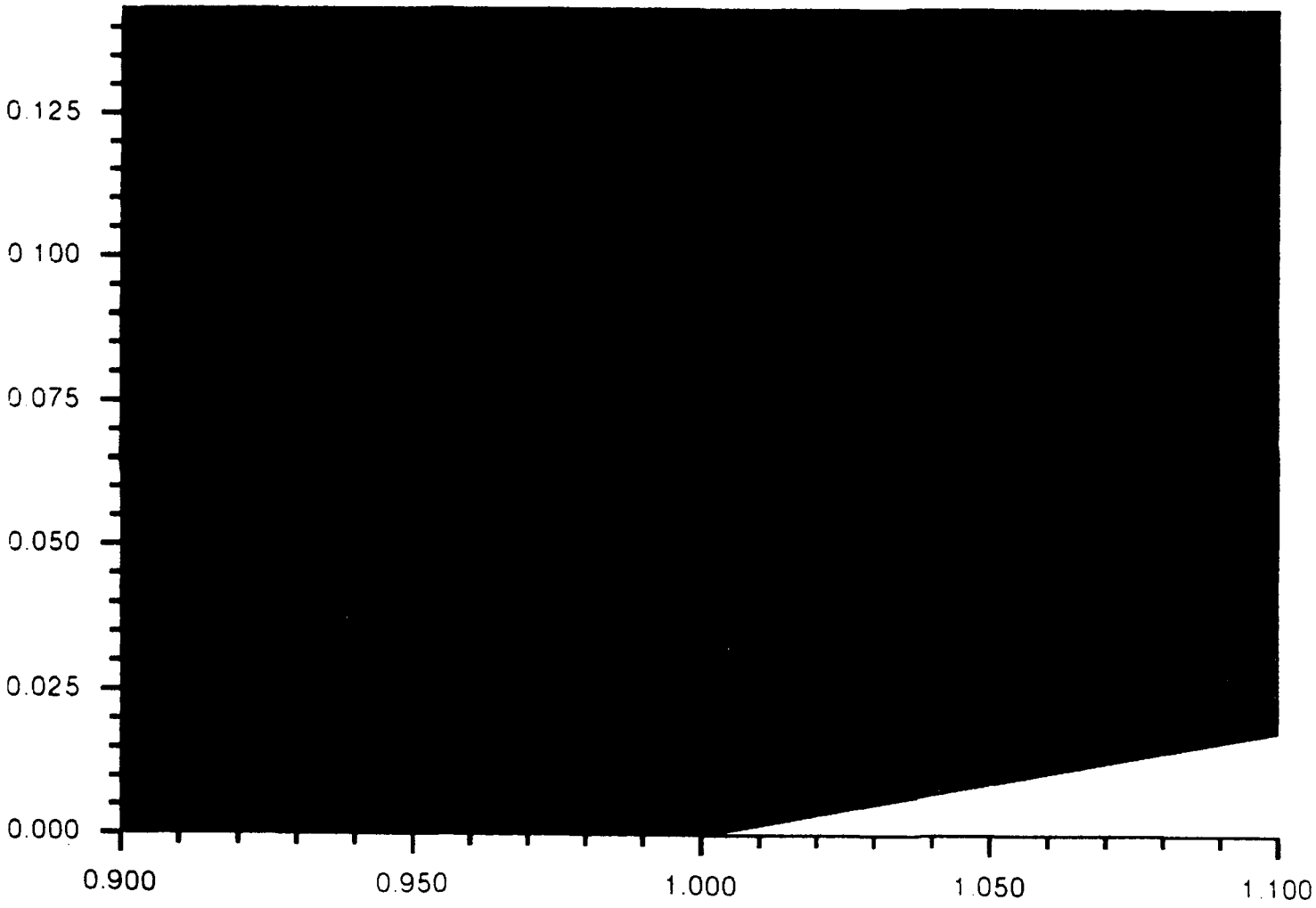

Figure 3b. Shock-boundary-layer interaction in compression corners at M = 6, Re = 15,000, cold wall

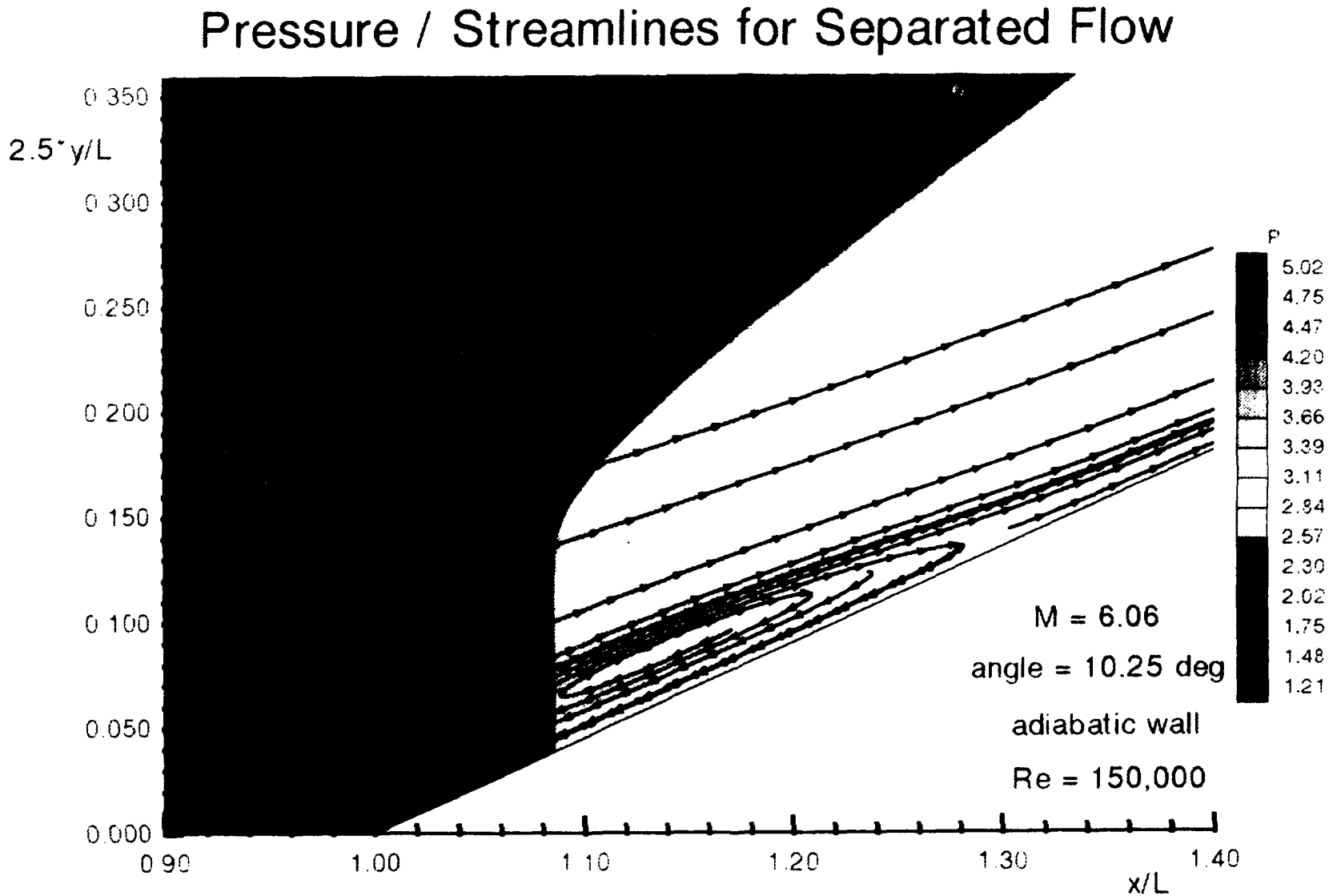

Figure 3c. Shock-boundary-layer interaction in compression corners at M = 6, Re = 150,000, hot wall

Fig 3d: RNS Results for Mach 3, 10 Degree Compression Corner

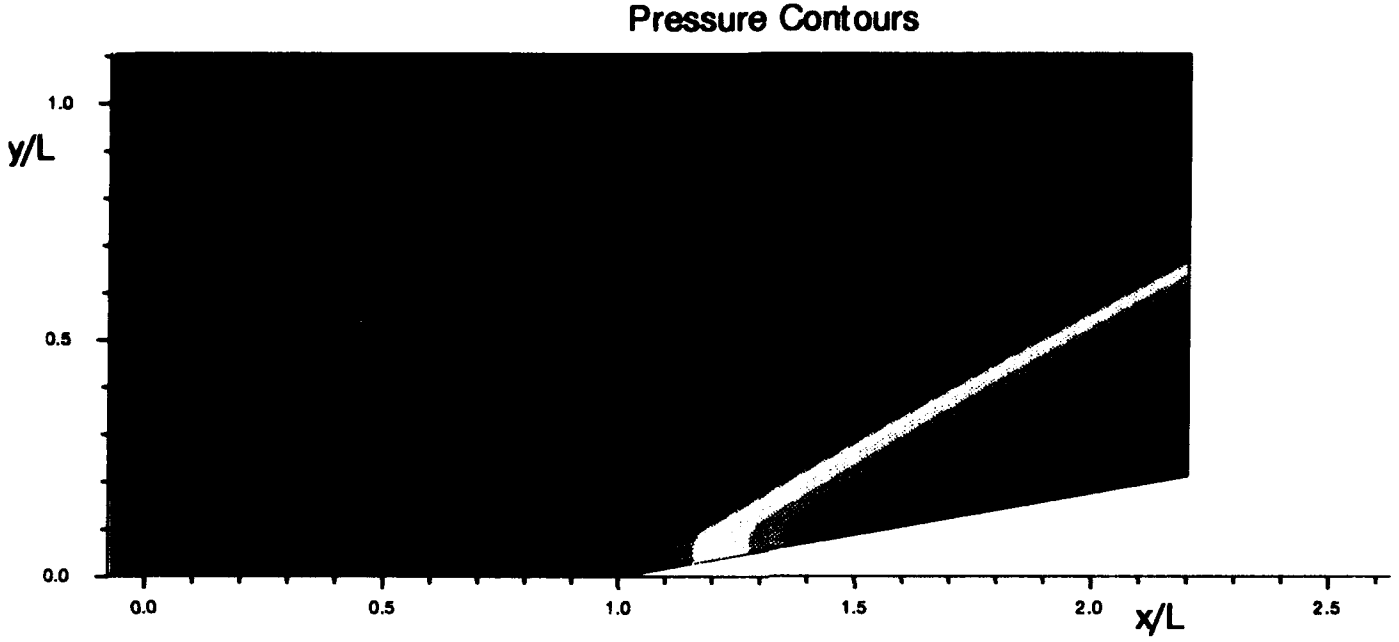

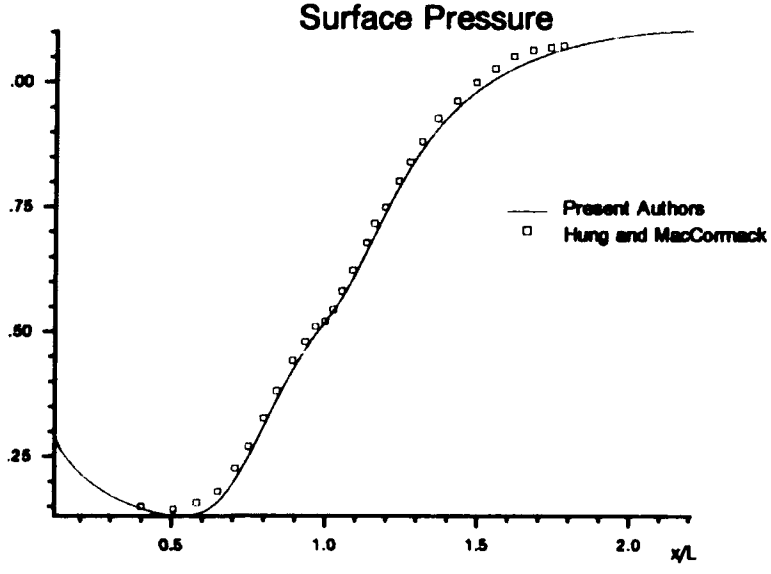

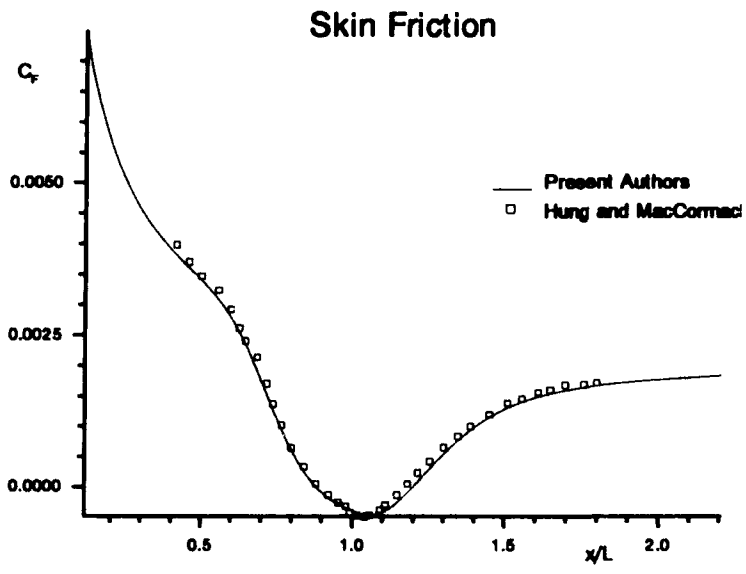

FIG 3e RNS Solution for Mach 14.1, 15 Degree Compression Corner

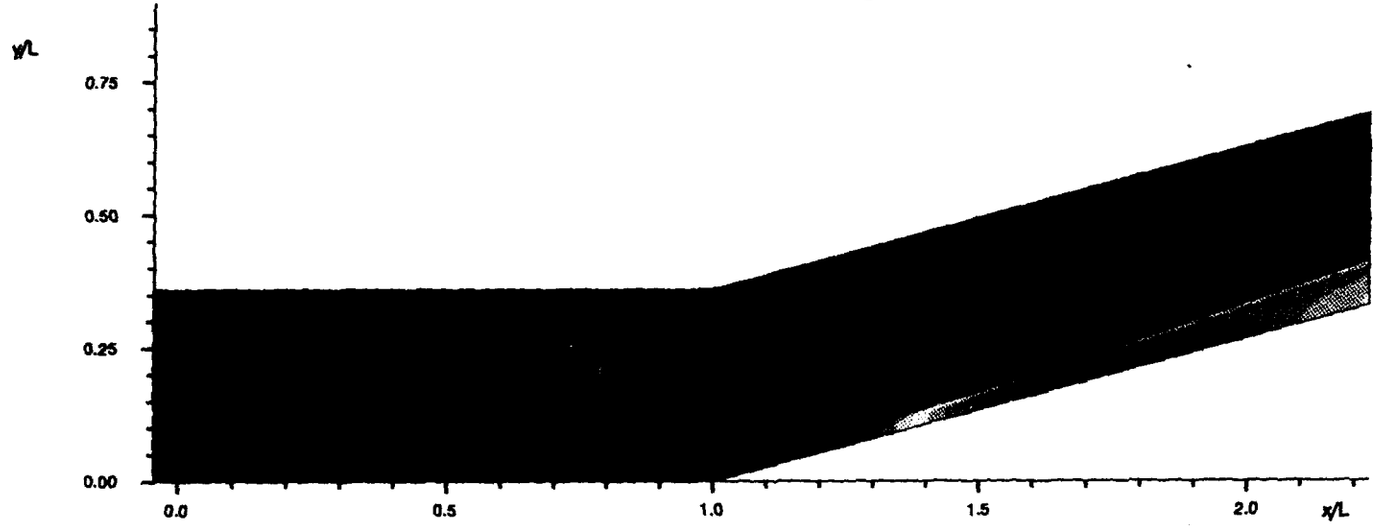

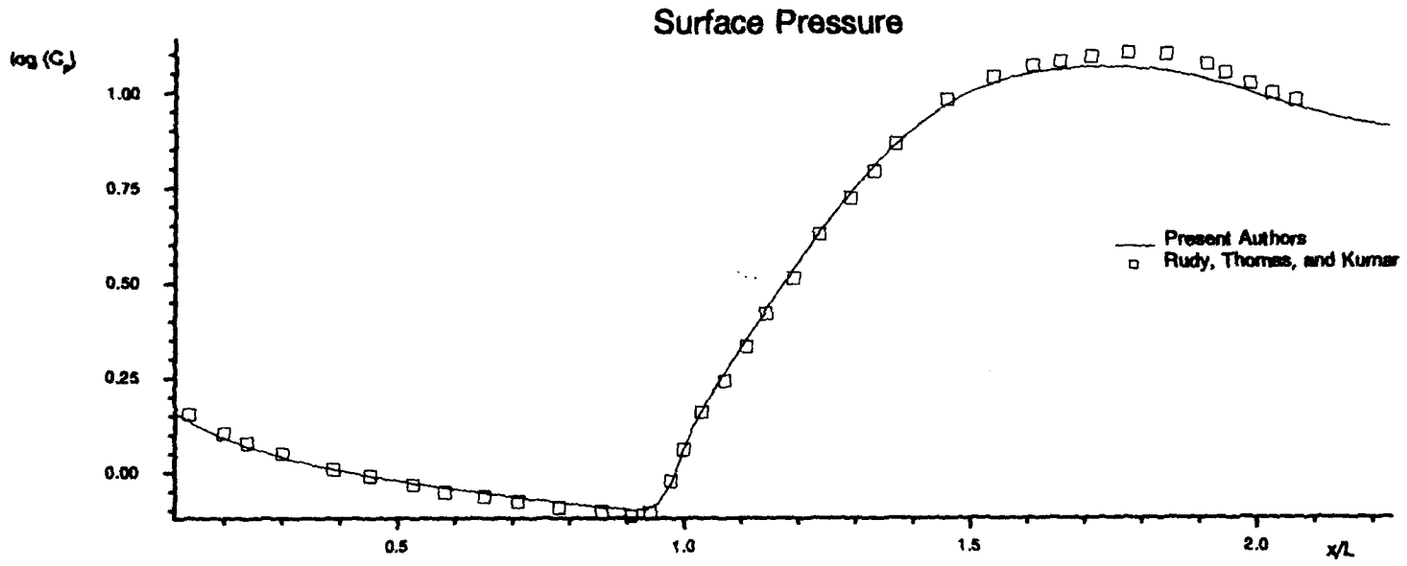

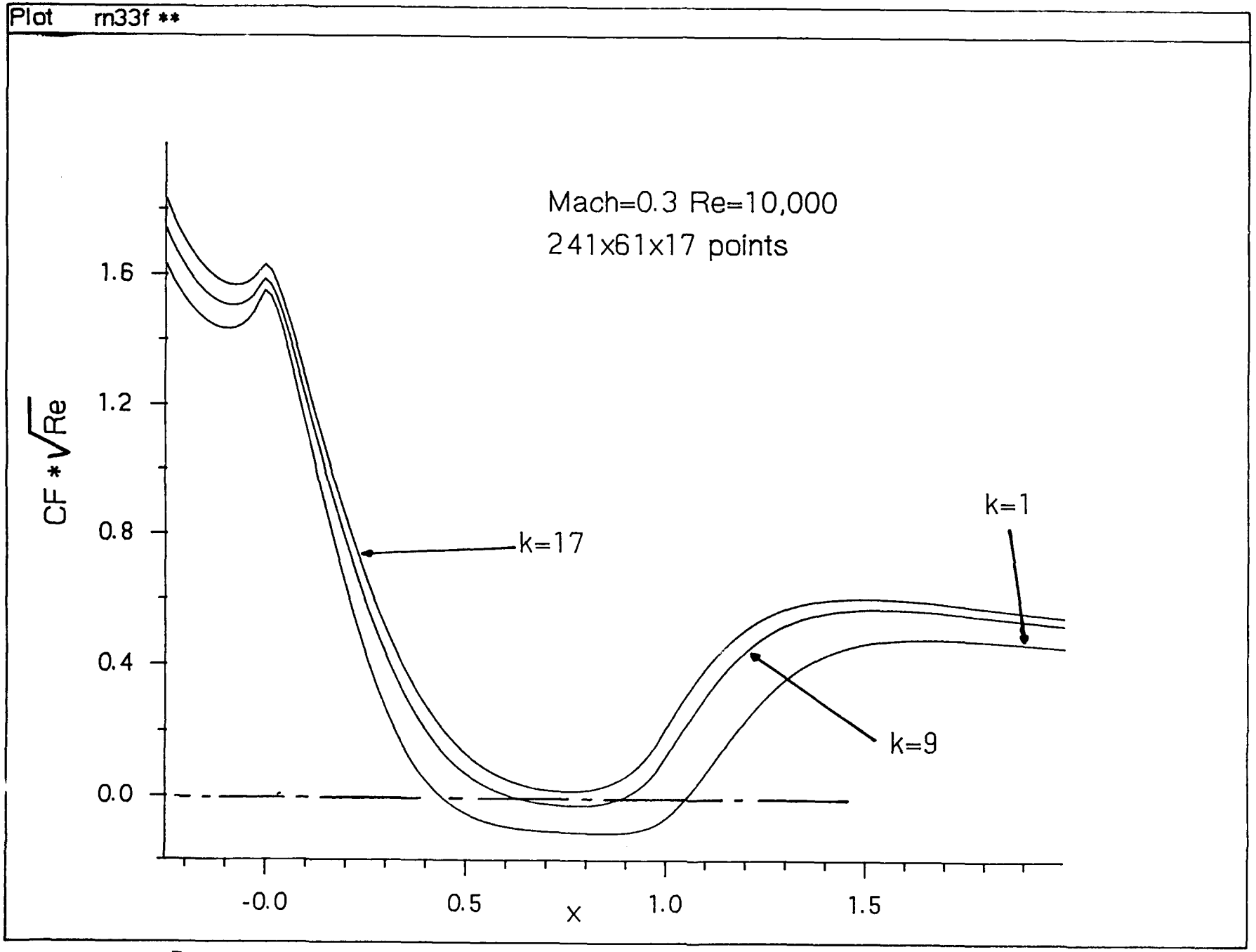

Figure 4a. High resolution 3-D separated flow

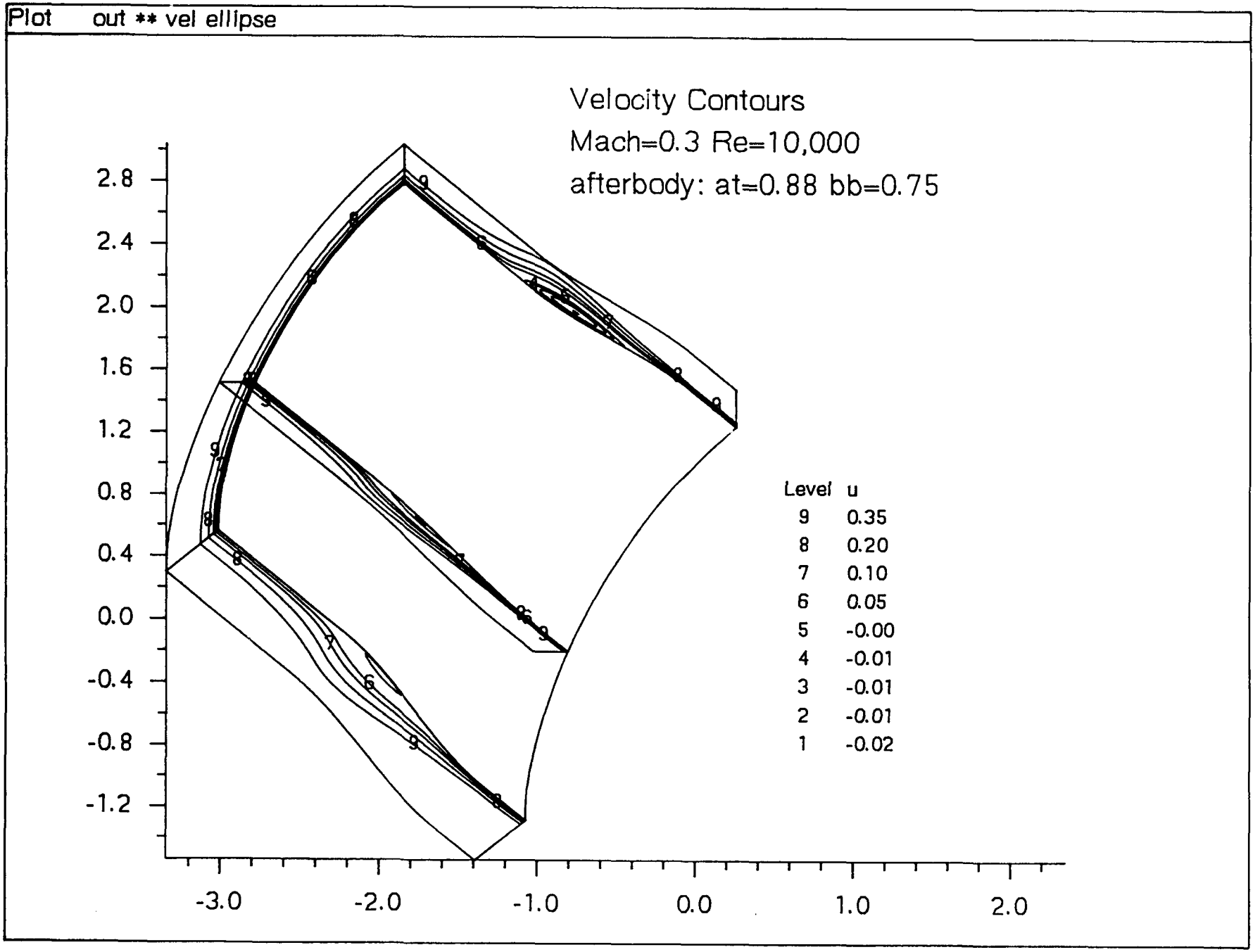

Figure 4b. High resolution 3-D skin friction on afterbody

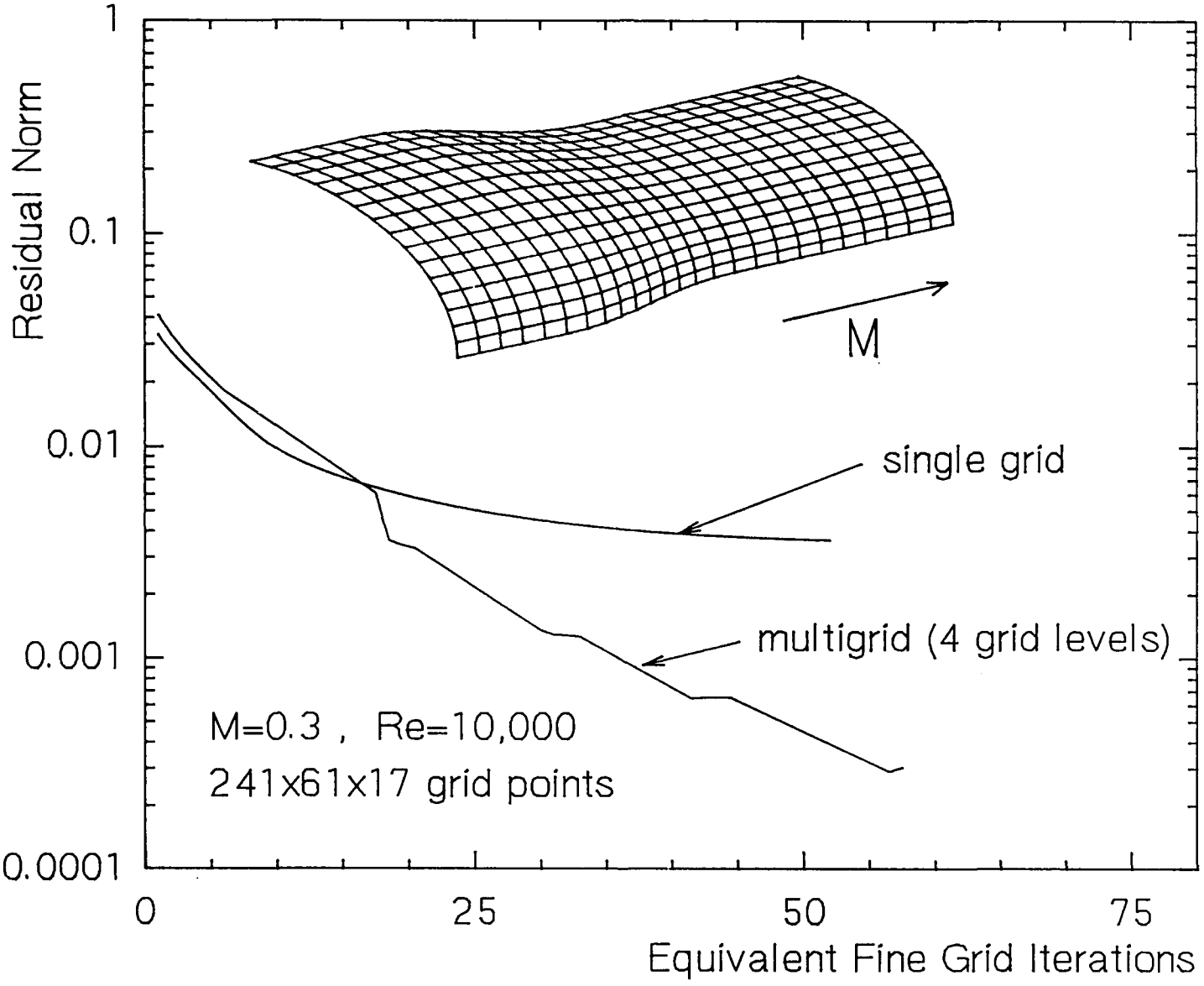

Figure 4c. Afterbody with Elliptic X-Section - Multigrid Convergence

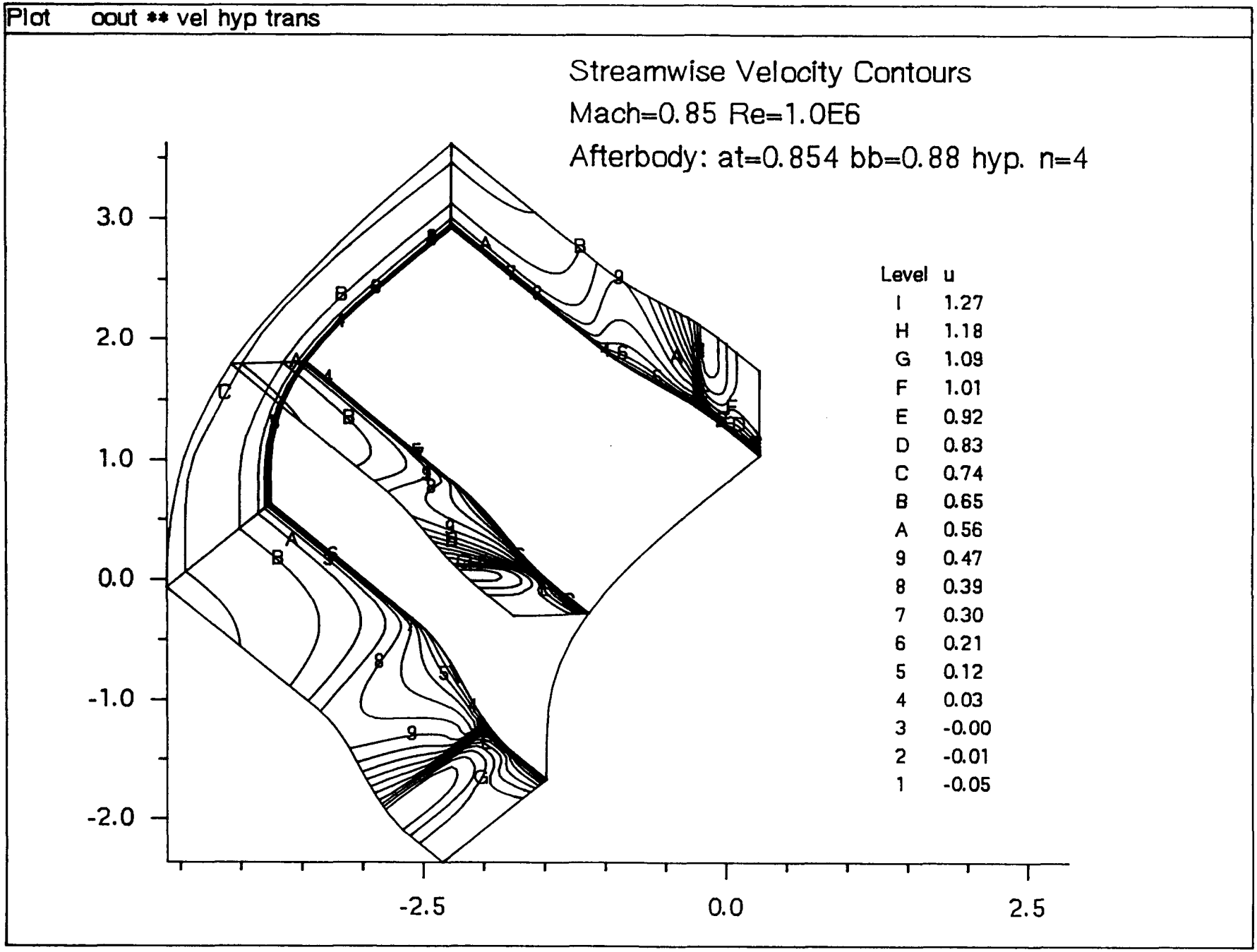

Figure 4d. Shock boundary-layer interaction M = .85, Re = 10^6 (turbulent)

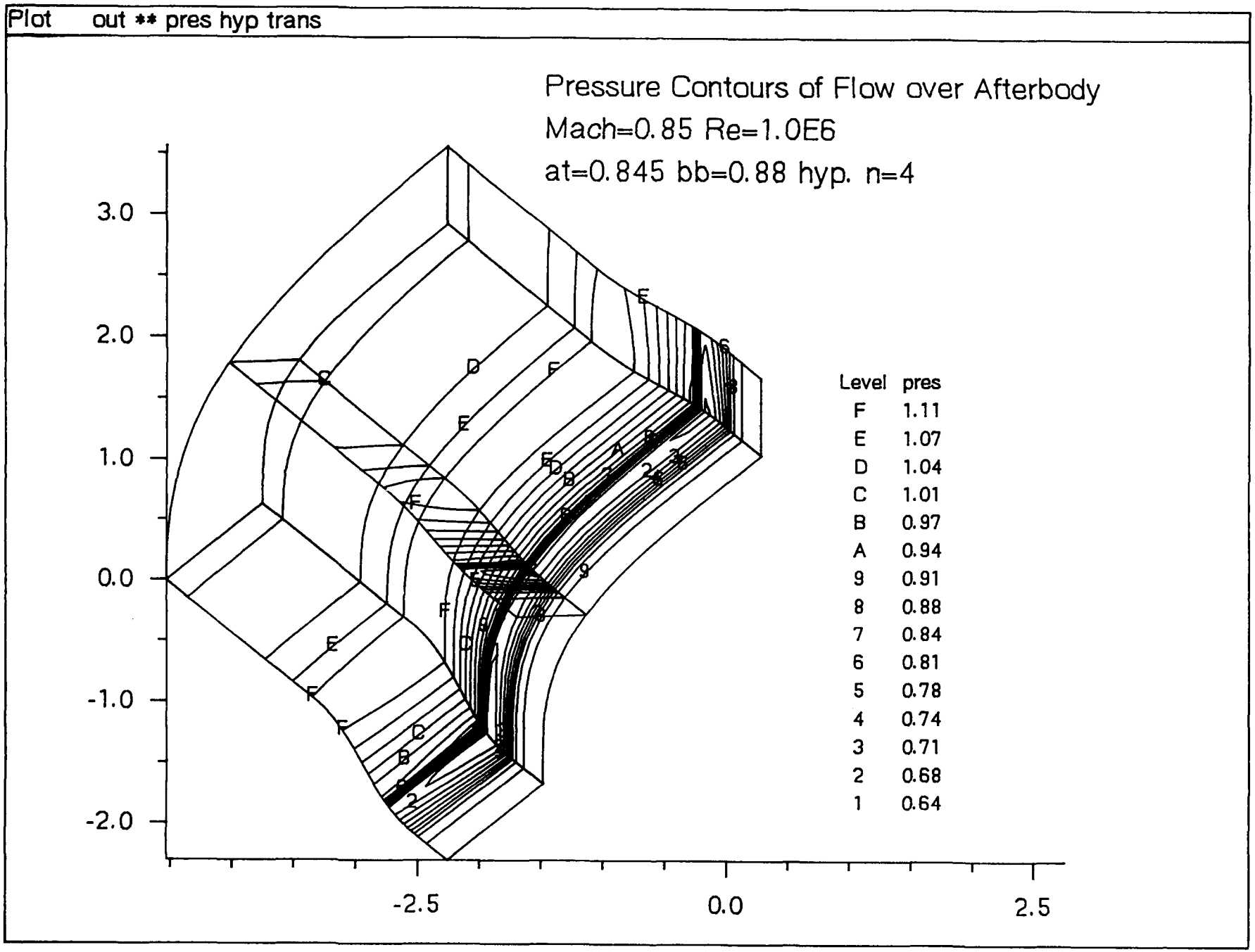

Figure 4e. Shock boundary-layer interaction (turtulent)

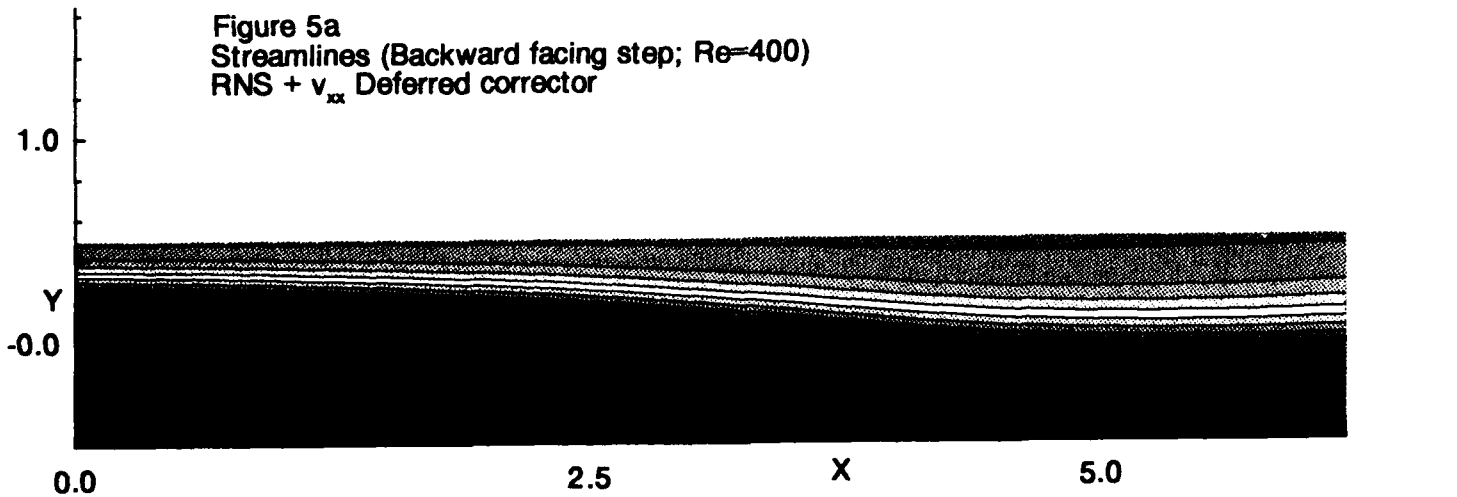
Figure 5a
Streamlines (Backward facing step; Re=400)
RNS + v_{xx} Deferred corrector
1.0
Y
-0.0
0.0
2.5
X
5.0

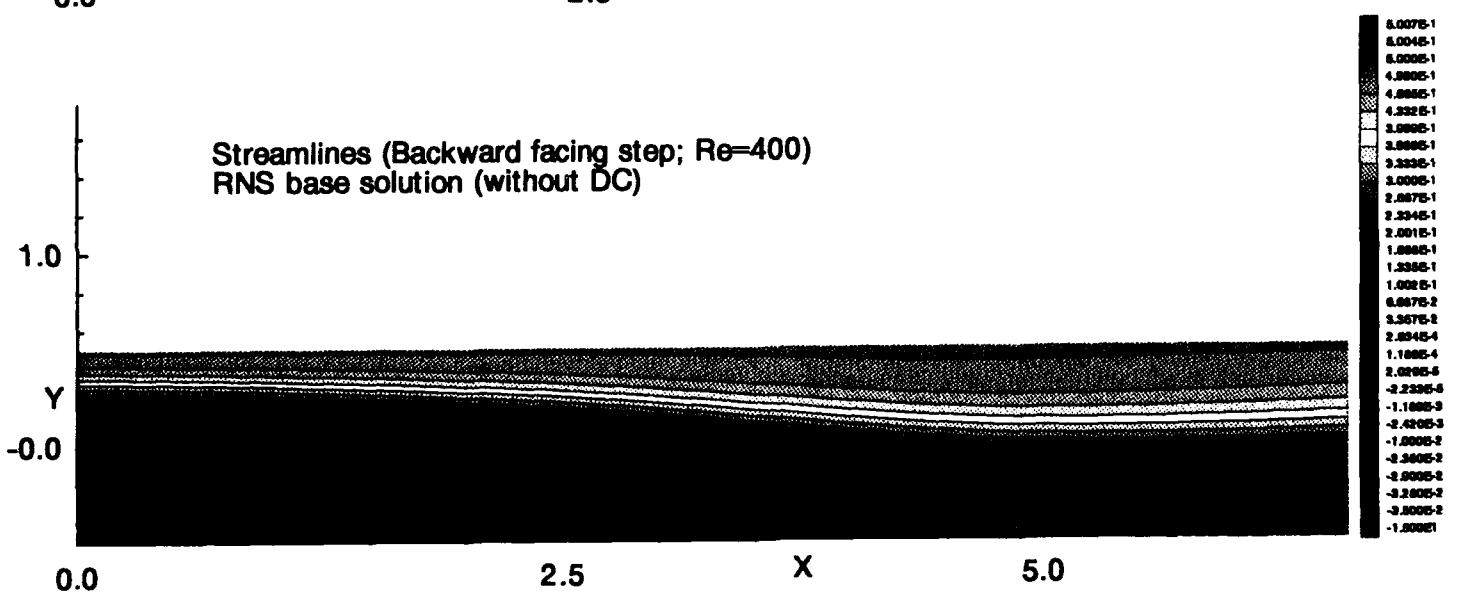
Streamlines (Backward facing step; Re=400)
RNS base solution (without DC)
1.0
Y
-0.0
0.0
2.5
X
5.0

Figure 5b. Effect of outflow boundary condition

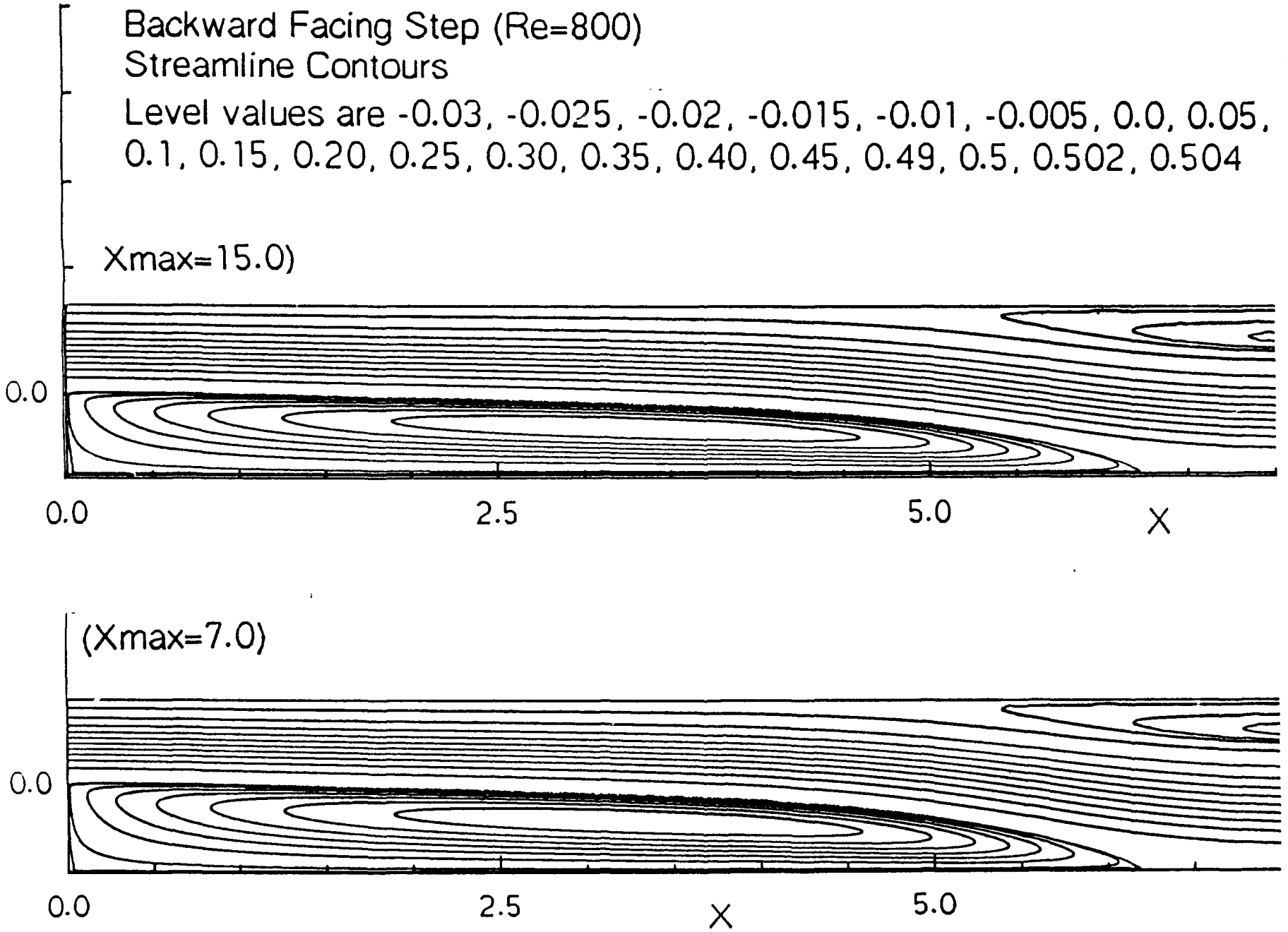

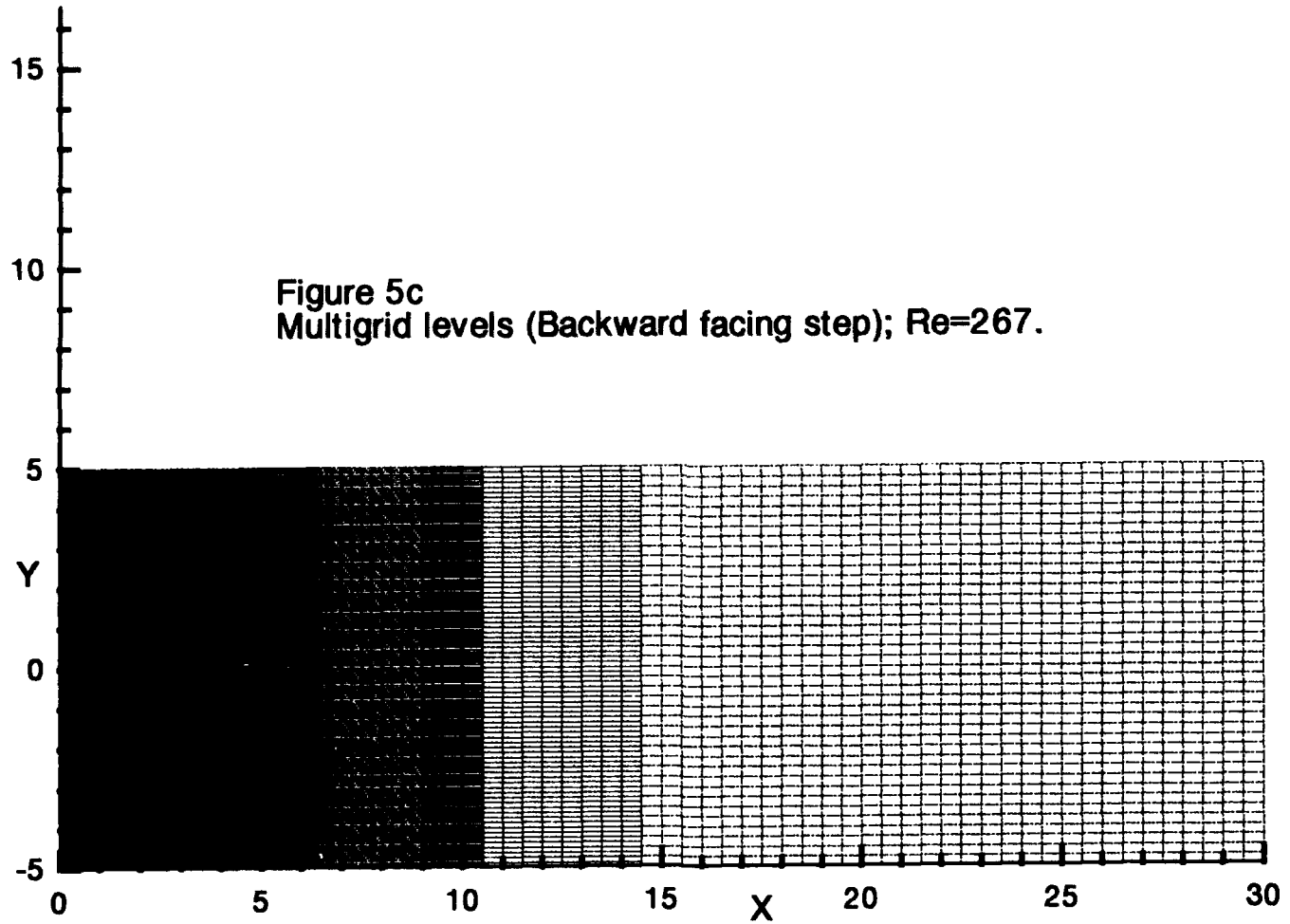

Figure 5c
Multigrid levels (Backward facing step); Re=267.

Figure 5d
Streamfunction Contours - Backward Facing Step (Re=800; Xmax=30.0)
Level values are -0.030, -0.025, -0.020, -0.015, -0.010, -0.005, 0.0, 0.05, 0.100, 0.150, 0.200, 0.250, 0.300, 0.350, 0.400, 0.450, 0.490, 0.500, 0.502, 0.504

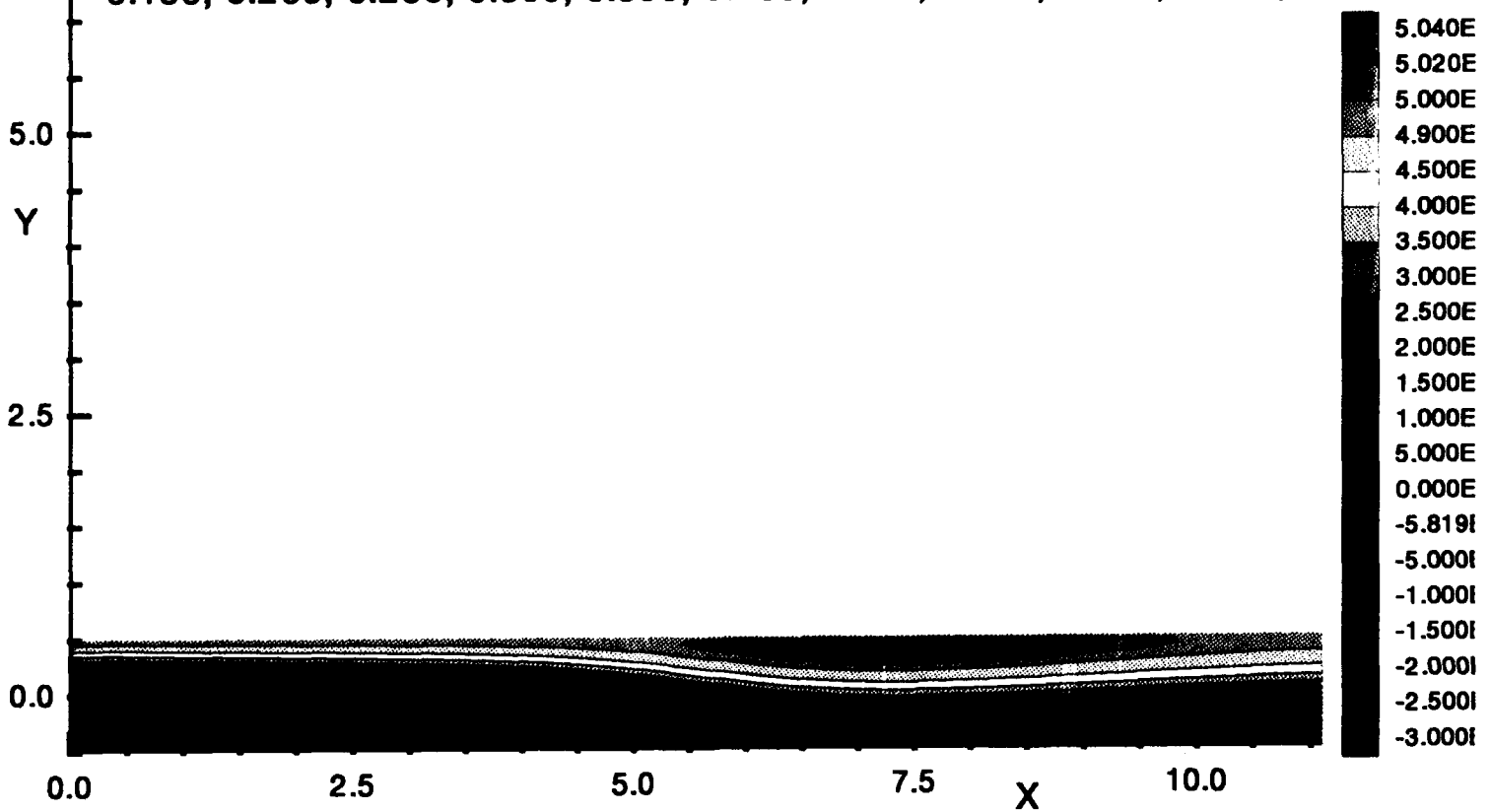

Figure 5e
Multigrid levels (Trailing edge flow; $Re=10^5$)

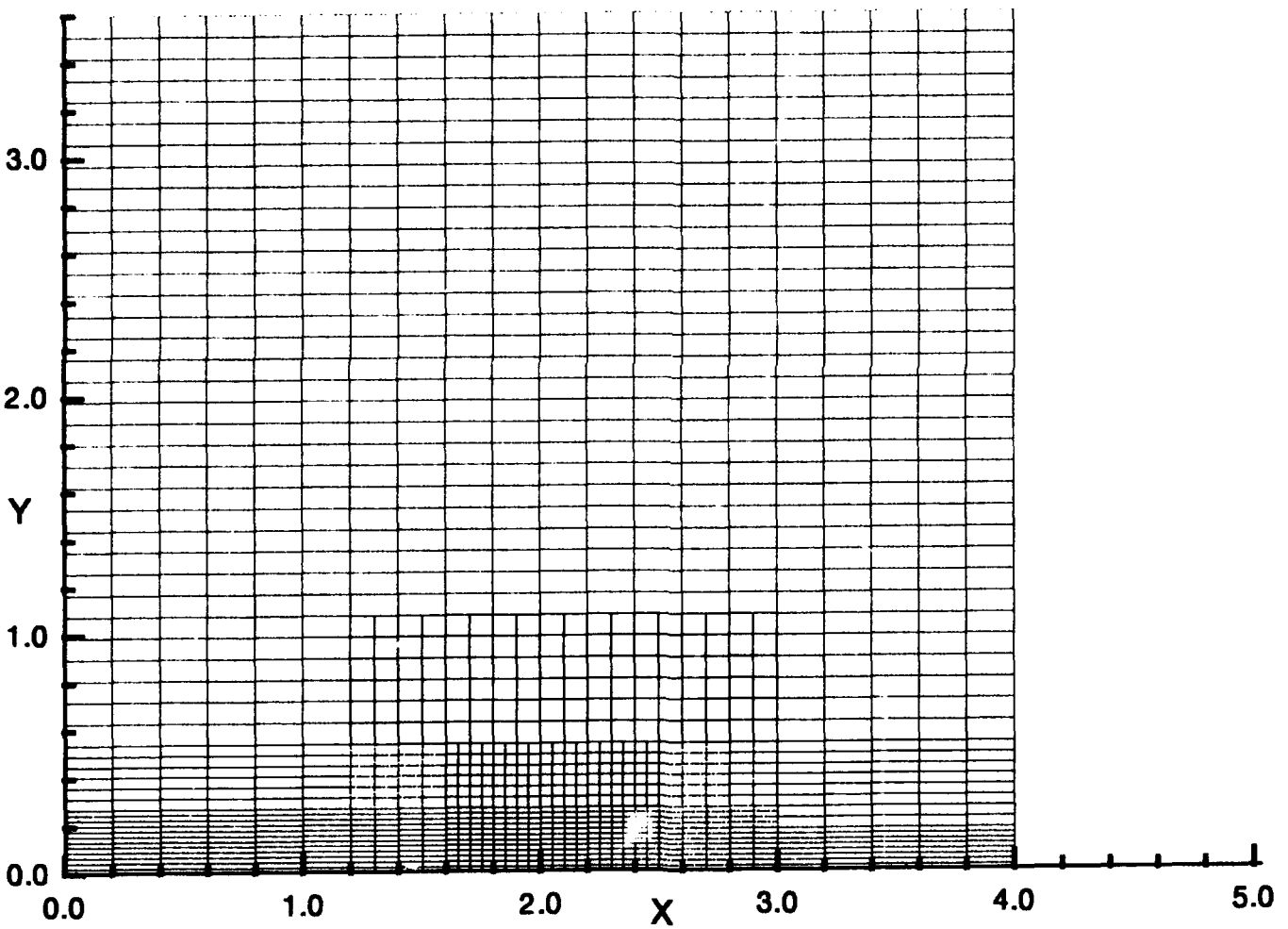

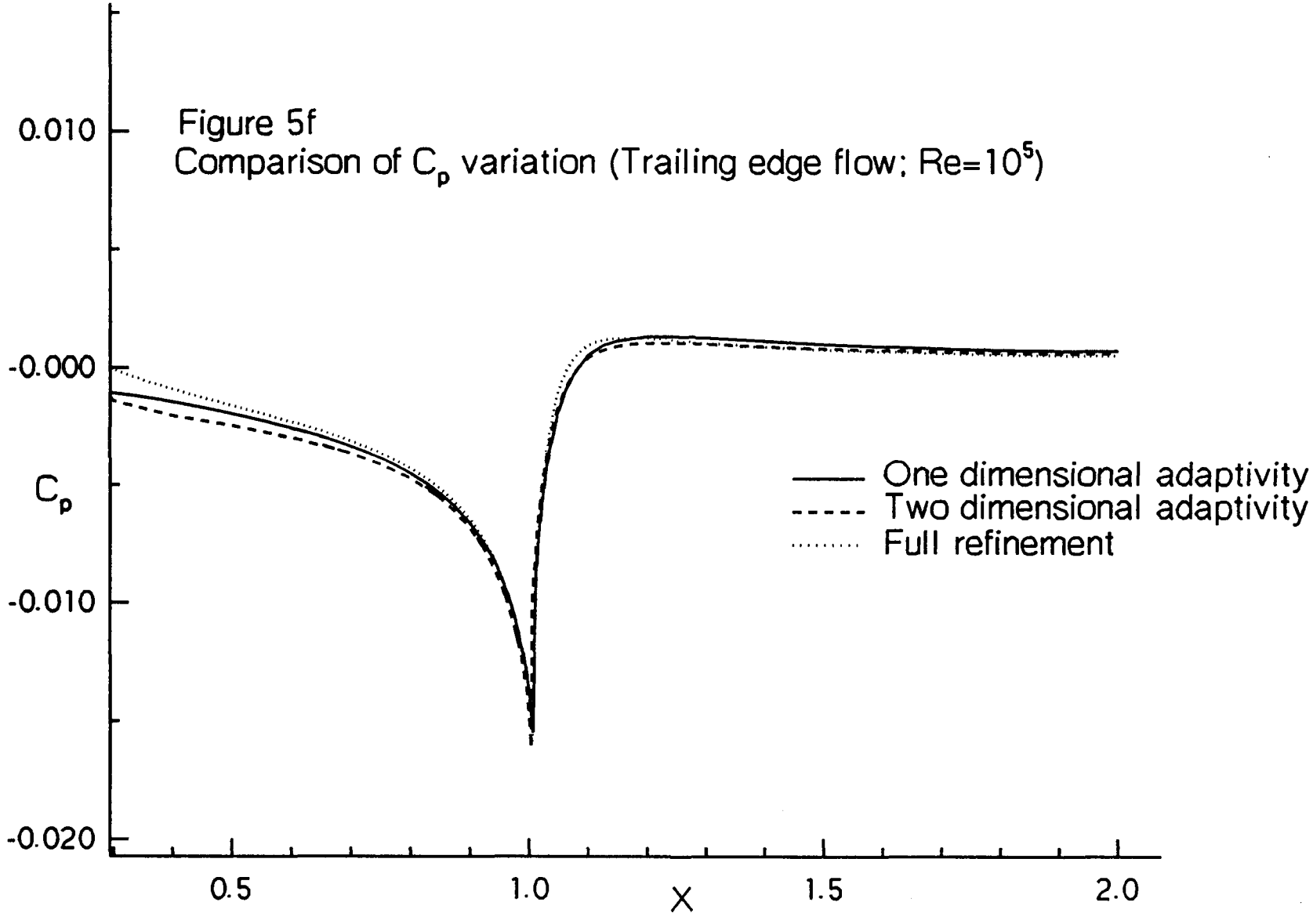
Figure 5f
Comparison of C_p variation (Trailing edge flow; $Re=10^5$)
0.010
-0.000
-0.010
-0.020
C_p
0.5
1.0
1.5
2.0
X
One dimensional adaptivity
Two dimensional adaptivity
Full refinement